

# **THE IMPACT OF FILTER LOADING ON RESIDENTIAL HVAC PERFORMANCE**

A Thesis  
Presented to  
The Academic Faculty

by

Abraham Kruger

In Partial Fulfillment  
of the Requirements for the Degree  
Masters of Science in Building Construction in the  
School of Building Construction

Georgia Institute of Technology  
December 2013

**Copyright 2013 by Abraham Kruger**

# **THE IMPACT OF FILTER LOADING ON RESIDENTIAL HVAC PERFORMANCE**

Approved by:

Dr. Javier Irizarry, Advisor  
School of Building Construction  
*Georgia Institute of Technology*

Dr. Brent Stephens  
Department of Civil, Architectural  
and Environmental Engineering  
*Illinois Institute of Technology*

Dr. Daniel Castro-Lacouture  
School of Building Construction  
*Georgia Institute of Technology*

Rick Porter  
School of Building Construction  
*Georgia Institute of Technology*

Date Approved: November 15, 2013

## **ACKNOWLEDGEMENTS**

This thesis would not have been possible without the generous support of my thesis committee, friends and family, test home volunteers, and numerous industry professionals. In no particular order, I would like to thank Abbey Kruger, Evonne Kruger, Isaak Kruger, Matt Laliberte, Carl Seville, Laura Capps, Terrel Broiles, Gary Nelson, Jeffrey Saules, Ela Orenstein, Georgia Hill, Roxanne Greeson, Kevin Thompson, Bob Mason, Eyu-Jin Kim, Jacquelyn Strickland, Lorie Wooten, and Amin Esmaeili.

I would also like to acknowledge the generous support of the National Housing Endowment who provided a Homebuilding Education Leadership Program (H.E.L.P.) grant to the School of Building Construction at Georgia Tech and through which I was able to pursue this research as a Residential Construction Industry Applied Research Fellow.

# TABLE OF CONTENTS

	Page
ACKNOWLEDGEMENTS	iv
LIST OF TABLES	viii
LIST OF FIGURES	ix
LIST OF SYMBOLS AND ABBREVIATIONS	xi
SUMMARY	xiv
<u>CHAPTER</u>	
1 Introduction	1
2 Literature Review	3
HVAC Prevalence	4
Heating and Cooling Systems	5
HVAC Motors	6
Types of Filters	7
Filter Efficiency	8
Coil Fouling	10
Pressures within HVAC Systems	11
Airflow within HVAC Systems	15
Filters Impact on Energy Consumption	18
3 Methodology	22
Research Design	22
Test House Selection	23
Filter Loading Simulation	25
Data Collection	27

	Fan Curve Determination Procedure	30
	Data Analysis	33
4	Field Results and Data Analysis	35
	Test System Descriptions	35
	Test System Locations	35
	Test System 1	36
	Test System 2	37
	Test System 3	38
	Test System 4	38
	Test Systems 5 and 6	39
	Analysis	40
	Filter Pressure Drop and System Airflow	40
	Filter Pressure Drop and Temperature	43
	Filter Pressure Drop and Absolute Humidity	47
	Airflow and Temperature	49
	Airflow and Absolute Humidity	52
	Airflow and System Capacity	54
5	Conclusion	60
	Filter Pressure Drop and System Airflow	60
	Filter Pressure Drop and Temperature	61
	Filter Pressure Drop and Absolute Humidity	61
	Airflow and Temperature	61
	Airflow and Absolute Humidity	62
	Airflow and System Capacity	62
	Analysis Summary	62

Recommendations	63
APPENDIX A: Field data from 6 test systems	64
REFERENCES	70

## LIST OF TABLES

	Page
Table 1: Stephens et al. results	20
Table 2: Test system characteristics	24
Table 3: Measurement type and location	31
Table 4: Testing instrumentation	31
Table 5: Filter pressure drop and system airflow	42
Table 6: Filter pressure drop and $\Delta T$	43
Table 7: Z-scores for each $\Delta T$ measurement	45
Table 8: Filter pressure drop and absolute humidity differences across the coil	48
Table 9: Filter pressure drop and $\Delta T$ across the evaporator coil	50
Table 10: System airflow and $\Delta W$ across the evaporator coil	52
Table 11: Relationship of airflow and sensible capacity for all systems	55
Table 12: Relationship of airflow and latent capacity for all systems	56
Table 13: Relationship of airflow and total capacity for all systems	57

## LIST OF FIGURES

	Page
Figure 1: U.S. energy use by sector	3
Figure 2: Air Conditioning equipment growth in the US	5
Figure 3: System and fan curves for medium-, high-, and low-pressure-drop filters	14
Figure 4: The Alnor EBT Balometer	16
Figure 5: TrueFlow® Air Handler Flow Meter	17
Figure 6: The research process.	22
Figure 7: Percent of new homes containing central air conditioners in the south	23
Figure 8: An example of a partially taped filter (“TrueFlow Taped 1”)	26
Figure 9: An example of a partially taped filter (“TrueFlow Taped 2”)	26
Figure 10: An example of a partially taped filter (“TrueFlow Taped 3”)	27
Figure 11: Vertical HVAC system with one central filter.	28
Figure 12: Horizontal HVAC system with one central filter.	29
Figure 13: Vertical HVAC system with two central filters.	30
Figure 14: The location of the 4 test homes in the Atlanta metro-region.	36
Figure 15: Test system 1	37
Figure 16: Test system 2	38
Figure 17: Test system 3	39
Figure 18: Test systems 5 and 6	40
Figure 19: Relationship of induced filter pressure drop and system airflow	41
Figure 20: System airflow versus filter pressure drop.	42
Figure 21: Relative $\Delta T$ across the coil versus filter pressure drop for each test system	46
Figure 22: Relationship of filter pressure drop and $\Delta T$ across all systems.	47
Figure 23: Relationship of filter pressure drop and $\Delta W$ for each test systems	48



Figure 24: Relationship of filter pressure drop and $\Delta W$ for all systems.	49
Figure 25: Relationship of airflow and $\Delta T$ for each system.	50
Figure 26: Relationship of airflow and $\Delta T$ for all systems.	51
Figure 27: The relationship of airflow and absolute humidity for each system	53
Figure 28: Relationship of airflow and absolute humidity for all systems.	54
Figure 29: Relationship of airflow and sensible capacity for all systems	55
Figure 30: Relationship of airflow and latent capacity for all systems.	56
Figure 31: Relationship of airflow and total capacity for all systems.	57

## LIST OF SYMBOLS AND ABBREVIATIONS

AC	Air conditioner
AC	Alternating current
ACCA	Air Conditioning Contractors of America
ACDX	Direct expansion AC
AHS	American Housing Survey
AHU	Air handling unit
ANSI	American National Standards Institute
ASHRAE	American Society of Heating, Refrigerating and Air-Conditioning Engineers
Btu/hr	British thermal units per hour
C	Celsius
C	Specific heat of air, kJ/kgK
$C_{\text{total}}$	Coefficient of proportionality for the entire system
$C_{\text{return}}$	Coefficient of proportionality for the return duct
$C_{\text{filter}}$	Coefficient of proportionality for the filter
$C_{\text{CC}}$	Coefficient of proportionality for the cooling coil
$C_{\text{HC}}$	Coefficient of proportionality for the heating coil
$C_{\text{S1}}$	Coefficient of proportionality for the first supply duct branch
$C_{\text{S2}}$	Coefficient of proportionality for the second supply duct branch
$C_{\text{S3}}$	Coefficient of proportionality for the third supply duct branch
CFM	Cubic feet per minute, ft <sup>3</sup> /min
COP	Coefficient of performance
DC	Direct current
DOE	Department of Energy
ECM	Electronically Commutated Motor also known as a Brushless DC Motor

EER	Energy Efficiency Ratio
EIA	Energy Information Administration
EST	Eastern Standard Time
F	Fahrenheit
g	Gram
$\eta_{fan}$	Efficiency of the fan
$h_{fg}$	Latent heat of vaporization for water, assumed constant, (970 Btu/lb)
HUD	Housing and Urban Development
HVAC	Heating, Ventilation and Air Conditioning
IAQ	Indoor air quality
ICC	International Code Council
IRC	International Residential Code
IWC	Inches of water column
k	Unit of measurement equal to 1,000
K	constant based on measured airflow and pressure
K	Kelvin
kWh	kilowatt-hours
$\eta_{motor}$	Efficiency of the fan motor
$m^3/s$	cubic meters per second
MERV	Minimum efficiency reporting value
$Q_{reference}$	Volumetric flow rate of air with measuring device installed, $m^3/hr$ (cfm)
P	System pressure, Pa (IWC)
$\rho$	Air density, $kg/m^3$
Pa	Pascal
PSC	Permanent split capacitor
Q	System airflow rate, $m^3/s$ (cfm)
$Q_{fan}$	Volumetric flow rate of air flowing across the fan, $m^3/s$ (cfm)

$s$	Standard deviation
VAV	Variable air volume
VOC	Volatile organic compound
W	Watts
W	Humidity ratio
$W_{fan}$	Power draw of fan, W
$Y_i$	Sample value
$\bar{Y}$	Sample mean
$\Delta P_{reference}$	Supply plenum pressure with measuring device installed, Pa (IWC)
$\Delta P_{operating}$	Operating supply plenum pressure, Pa (IWC)
$\Delta T$	Temperature difference across the cooling coil, K (°F)
$\Delta W$	Humidity ratio difference across the cooling coil, kg/kg

## SUMMARY

Residential and commercial buildings account for approximately 41% of total energy use in the US. Within households, approximately 50% of total energy use is associated with space heating and cooling. Heating, ventilation, and air-conditioning (HVAC) systems are designed to provide occupant comfort by meeting heating and cooling loads safely and efficiently. Air cleaning devices, particularly particle air filters, are important components of HVAC systems that prevent damage to HVAC equipment and improve indoor air quality (IAQ) by reducing airborne particle concentrations. HVAC filters, however, can also have significant impacts on the performance of HVAC equipment in both residential and commercial buildings.

Coil fouling, or the deposition of airborne particles on the evaporator coil inside an HVAC system's air handling unit (AHU), will increase system pressure drop and reduce heat transfer effectiveness, which decreases airflow and air conditioner (AC) performance. Although filters can increase AC performance by decreasing coil fouling, filters may also have energy implications, particularly if they are higher pressure drop filters or if they become dirty (or "loaded") over time. In large commercial HVAC systems with variable speed blowers, energy implications are simple: fans will simply draw more power to overcome a greater pressure drop to deliver the same amount of required cooling. In smaller residential systems without sophisticated airflow controls, recent research has shown that as filters become loaded, pressure drop across the filter increases and airflow is restricted. Cooling systems should therefore run longer as airflow is reduced to provide adequate cooling at the reduced capacity, although little quantitative information exists on the magnitude of the impacts of filter pressure drop on airflow rates, cooling capacities, and system runtimes in real residential systems. Complicating the issue is that while most homes currently have inefficient blowers without flow controls (i.e., permanent split capacitor, or PSC, motors), new AHU products on the

market utilize more sophisticated fans with flow controls (i.e., those with electrically commutated motors, or ECM, blowers, also called brushless permanent magnet, or BPM, blowers).

Therefore, the following report reviews recent research on HVAC filters for central forced-air air-conditioning units and electric heat pumps and presents the findings of an in-situ evaluation of AC performance under simulated filter loading conditions. The study hypothesized that it was possible to develop a methodology for simulating filter loading in-situ that would allow for the observation of the impact of filter loading on AC performance in-situ and provide a greater understanding of when a filter is “dirty” and thus inform when it should be replaced.

Six central AC systems in the Atlanta metro-region were evaluated in this work. Several conditions of filter loading were artificially induced in the test systems and filter pressure drops, airflow rates, temperature and humidity differences across the coil were all measured during pseudo-steady-state cooling operation, which allowed for developing relationships between simulated filter loading, airflow, and sensible and latent capacity. Filter loading was simulated by installing an Energy Conservatory TrueFlow® plate airflow metering device and partially taping off the face at three different increments. This resulted in measurements at 5 discrete static pressure conditions: no filter, TrueFlow measurement, TrueFlow Taped #1, TrueFlow Taped #2, and TrueFlow Taped #3, increasing in simulated filter pressure drop at each increment. These in-situ measurements revealed that as filter pressure drop increased, airflow rates generally decreased, particularly for the known PSC blowers, as is expected from the literature. Two of the test systems were apparently ECM blowers as they responded to increased filter pressure drop by nearly maintaining airflow rates until reaching a maximum pressure and rapidly decreasing in flow, which is consistent with other ECM data. Therefore the data herein are considered generally representative of both types of systems, even with a limited data set.

With moderate certainty, it was found that as induced filter pressure drop increased, the difference in temperature across the evaporator coil ( $\Delta T$ ) also increased in these systems. These data support what other laboratory and field studies have shown: as airflow rates are reduced in the presence of larger filter pressure drops, sensible capacity will not decrease linearly with flow because the temperature difference across the coil increases slightly and supply air is delivered at a lower temperature. This data also shows that there is a stronger relationship between coil  $\Delta T$  and airflow as opposed to  $\Delta T$  and induced filter pressure drop, as filter pressure drop did not impact airflow rates uniformly in the systems.

There was no observed correlation between absolute humidity differences across the evaporator coil ( $\Delta W$ ) and either filter pressure drop or system airflow rates. In other words, as airflow decreased so did sensible, latent, and total capacity, although these relationships were not linear. Because reductions in cooling capacity can be linked to increased system runtimes, this research can be used to inform decisions about maximum filter loading values that should inform filter replacement schedules. Once a maximum acceptable reduction in sensible capacity is established, this data can be used to identify the airflow and filter pressure drop thresholds, which can impact future decisions about filter replacement timing.

This relatively limited pilot study provides valuable proof of concept for an approach to simulating in-situ filter loading and characterizing associated capacity impacts. Taping the face of the TrueFlow plate was shown to work consistently well to simulate filter loading. In the future, this study should be expanded to a greater number of central air conditioning units and continuous measurements should be recorded using data loggers, as one challenge was determining exactly when the AC systems reached steady state. Greater certainty may be possible by recording continuous measurements and waiting longer between each simulated filter condition.

# **CHAPTER 1**

## **INTRODUCTION**

Buildings account for approximately 41% of total energy use in the US (US Energy Information Administration 2011). Within households, approximately 50% of total energy use is for providing heating and cooling. Heating, ventilation, and air-conditioning (HVAC) systems are designed to provide occupant comfort safely and efficiently. HVAC systems control the indoor environment by heating, cooling, recirculating, and filtering the air and managing humidity. When not properly designed, installed, and/or maintained, these systems can increase energy consumption while compromising indoor air quality (IAQ).

Air cleaning devices, particularly particle air filters, are important components of HVAC systems that prevent damage to HVAC equipment and improve indoor air quality (IAQ) by reducing airborne particle concentrations. HVAC filters, however, can also have significant impacts on the performance of HVAC equipment in both residential and commercial buildings. Coil fouling, or the deposition of airborne particles on the evaporator coil inside an HVAC system's air handling unit (AHU), will increase system pressure drop and reduce heat transfer effectiveness, which decreases airflow and air conditioner (AC) performance. Although filters can increase AC performance by decreasing coil fouling, filters may also have energy implications, particularly if they are higher pressure drop filters or if they become dirty (or "loaded") over time. In large commercial HVAC systems with variable speed blowers, energy implications are simple: fans will simply draw more power to overcome a greater pressure drop to deliver the same amount of required cooling. In smaller residential systems without sophisticated airflow controls, recent research has shown that as filters become loaded, pressure drop across the filter increases and airflow is restricted. Cooling systems should therefore run longer as airflow is reduced to provide adequate cooling at the reduced capacity, although



little quantitative information exists on the magnitude of the impacts of filter pressure drop on airflow rates, cooling capacities, and system runtimes in real residential systems. Complicating the issue is that while most homes currently have inefficient blowers without flow controls (i.e., permanent split capacitor, or PSC, motors), new AHU products on the market utilize more sophisticated fans with flow controls (i.e., those with electrically commutated motors, or ECM, blowers, also called brushless permanent magnet, or BPM, blowers).

To date, studies on the impact of filters on residential HVAC system performance have used: (i) laboratory test systems (Siegel et al. 2002, Palani et al 1992); (ii) computer simulation models (Nassif 2012); (iii) small samples of 2-16 systems in-situ (Chimunk and Sellers 2000, Stephens et al 2012, Rodriguez et al 1996); and (iv) some combination of these three methods (Yang et al 2004).

## **Research Objectives**

The study hypothesized that it was possible to develop a methodology for simulating filter loading in-situ that would allow for the observation of the impact of filter loading on AC performance in-situ and provide a greater understanding of when a filter is “dirty” and thus inform when it should be replaced. In-situ data can then be used to evaluate and update computer simulation models as well as increase the model of knowledge of actual HVAC performance in residences.

## CHAPTER 2

### LITERATURE REVIEW

The U.S. Energy Information Administration (EIA) publishes the Annual Energy Review. The report includes data on: total energy production, consumption, and trade for petroleum, natural gas, coal, electricity, nuclear energy, renewable energy, and international energy; and financial, and environmental indicators. According to the most recent edition, buildings account for approximately 41% of total energy use in the US as shown in Figure 1 (US EIA 2011).

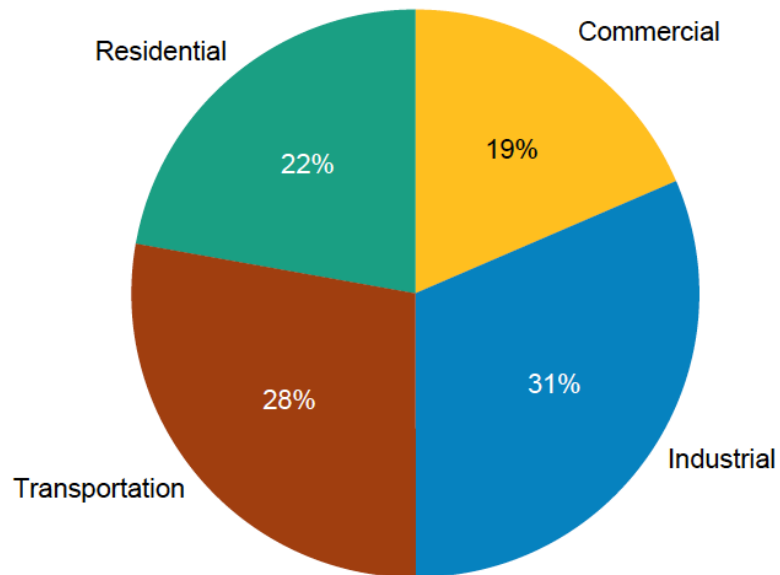


Figure 1. U.S. energy use by sector (US EIA 2011)

In 2005, US households consumed 0.88 quadrillion Btus and spent \$25.26 billion dollars on electricity for air conditioning (US EIA 2011)<sup>1</sup>. In that same year, US

---

<sup>1</sup> The 2005 data is what is available in the most recent Annual Energy Review from the DOE/EIA.

households consumed 0.28 quadrillion Btus and spent \$7.42 billion dollars on electricity for heating purposes. Even a slight improvement in heating and cooling system performance would result in significant energy consumption reductions across the residential building stock.

## **HVAC Prevalence**

Most homes require space conditioning, defined as heating, cooling, or both, depending on the local climate. The International Residential Code (IRC, the “building code”) requires that dwellings in cold climates contain heating equipment that can maintain indoor temperature at a minimum of 68°F (ICC 2012). There is no code requirement for cooling equipment in any US climate, although central air-conditioning is become ubiquitous in warmer climates.

The American Housing Survey for the United States (AHS) is sponsored by the U.S. Department of Housing and Urban Development (HUD) and conducted by the U.S. Census Bureau. National data is collected every 2 years and provides the most comprehensive national housing survey in the United States. The data covers a range of housing types, including single family, manufactured housing, and multifamily housing; and housing and resident characteristics, such as family composition, income, housing quality, neighborhood quality, housing costs, equipment, and fuel type. The most recent data from 2009 was published in 2011 (U.S. Census Bureau 2009).

Based on the most recent AHS, there are a total of 130,112,000 housing units, ranging from single family to multifamily and owner occupied to rental in the U.S. Approximately 1.5% of these dwellings are seasonal properties. The median dwelling was constructed in 1974 and contains 1,700 square feet. Approximately 63% of all American dwellings contain central AC for a total of 82,475,000 central AC units. Electric heat pumps are the primary heat source for 12% of American dwellings for a total of 16,059,000 heat pumps. Figure 2 shows the growth of AC systems within the

U.S.

**Air-Conditioning Equipment, 1980 and 2009**

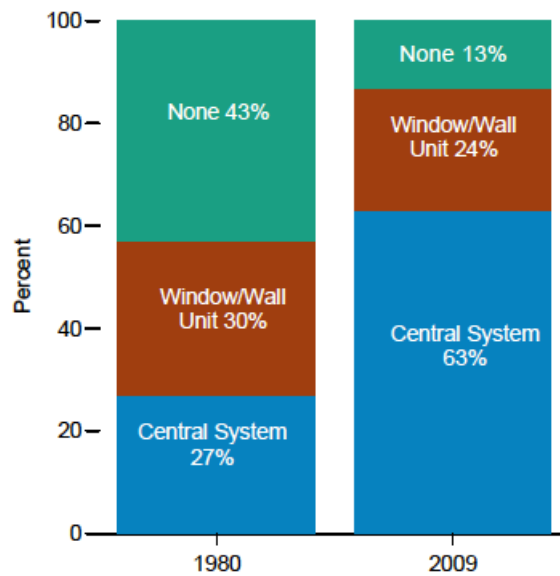


Figure 2. Air-conditioning equipment growth in the US (U.S. Census Bureau 2009).

US energy consumption for cooling is increasing as more homes are constructed with air conditioning systems. Thus, the importance of central AC system performance is also increasing.

### **Heating & Cooling Systems**

The key components of HVAC systems are the equipment used to supply energy for heating or extract energy for cooling, the fuel sources, and the method used to distribute the heating and cooling throughout the house. In forced-air systems, heated and cooled air is delivered by bulk convection into spaces that need heating or cooling. Individual systems that serve multiple areas of the home are referred to as whole-house systems, and those that serve only sections or single rooms are called local or non-distributed systems. Either of these can provide heating only, cooling only, or both, depending on the system type and climate requirements. Fuels can be fossil fuels (e.g.,

gas or oil), electricity, wood, or, in some cases, solar energy can be employed. Selecting the most appropriate distribution system and equipment, combined with proper design and installation, are critical to creating an effective and efficient HVAC system.

Central AC systems and heat pumps consist of a compressor and two coils made of copper or aluminum tubing (typically one located inside and one outside) that are surrounded by aluminum fins to aid heat transfer. Refrigerant, a chemical compound that transfers heat as it changes from a liquid to a gas and back, flows back and forth between the indoor and outdoor coils. The compressor, located outdoors, is a mechanical pump that increases the refrigerant pressure, raising its temperature. In a conventional AC system during cooling operation, the indoor evaporator coil serves to evaporate the refrigerant, changing its phase from a liquid to a gas, which absorbs energy from the air passing over the coil and thereby cools the airstream. Refrigerant is then piped to the condenser unit and heat is rejected to the outside, which acts as a heat sink. Humidity is also removed from the warm airstream as it passes over the cooler evaporator coil. Moisture leaves the vapor phase and is removed from the air as liquid water and drained to the exterior or a sewer system. Heat pumps operate similarly in the cooling mode.

In the heating mode, heat pumps operate in reverse. The outdoor condenser unit acts as an evaporator coil whereby liquid refrigerant in the outdoor unit extracts heat from the outdoor air and evaporates into a gas. The indoor coil now acts as a condenser and rejects heat into the indoor environment as it condenses back into a liquid. A reversing valve, near the compressor, can change the direction of the refrigerant flow for cooling as well as for defrosting the outdoor coil in winter.

## **HVAC Motors**

Electric motors are classified as either alternating current (AC) or direct current (DC) motors. AC motors are further broken down by the number of phases and whether they are synchronous or asynchronous (induction) motors. Approximately 90%

residential fans are permanent split-capacitor (PSC) (Sachs et al 2002), which do not have flow controls to maintain specified airflow rates. These fractional horsepower, AC induction motors usually have multiple speed windings, are low cost and tend to be 55% efficient under full-load (Murray 2012), although electric efficiencies measured in-situ are often much lower (Stephens et al 2010).

The most common alternative to PSC motors is electronically commutated motors (ECM), also called brushless permanent magnet (BPM) blowers. Unlike PSC motors, ECMs are able to adjust voltage levels to optimize motor torque as rotational speed is reduced. For these reasons, ECM motors tend to be much more efficient than comparably sized PSC motors, especially at low rotational speeds. They are also typically installed with flow controls that allow systems to maintain airflow rates in the presence of higher pressure drops. While ECM motors are more efficient, they also are more expensive due to the permanent magnets employed and additional circuitry.

Different HVAC operation modes require different airflows, which require varying blower motor speeds. Blower fan speeds for heat pump and air-conditioning modes are typically higher than a fan-only mode where no cooling or heating is being performed. Fan speeds are selected by the HVAC control system based on the particular mode of operation. Motor efficiency may vary based on fan speed. For example, unlike PSC motors, the efficiency of ECMs tends to increase as fan speed slows. Test results suggest that, on average, ECM motors represent a 51 percent full-load efficiency improvement over PSC motors (Murray 2012).

### **Types of Filters**

Air filtration devices, including particle air filters, are used to protect HVAC equipment from damage and coil fouling and to reduce concentrations of airborne particulate matter in indoor environments. Filters are normally installed as part of a forced-air HVAC system. The three primary types of filters are mechanical, pleated, and

electronic. The most common type used in homes, mechanical air filters, uses synthetic fibers or fiberglass to remove particles as they pass through the filter media. Pleated air filters are more effective than other mechanical air filters because they contain more fiber per square inch than mechanical filters. Electronic air filters use electricity to attract oppositely charged particles to metal fins. The particle removal efficiency of mechanical and pleated filters often improves as they become dirty because smaller and smaller particles are captured in the increasingly fine openings and loaded dust acts to increase effective fiber area (Earnest et al 2001). The effectiveness of electronic filters typically decreases over time without cleaning because the metal fins become ineffective when loaded. Filters may be installed at the air handling unit, return register, or as separate stand-alone equipment. This study focuses on filters installed at the air handling unit, as is common in many homes.

### **Filter Efficiency**

ANSI/ASHRAE Standard 52.2-2007 is used to address the ability of filtration devices to remove particles from the airstream and measure their resistance to airflow (ANSI/ASHRAE 2007). Here, efficiency refers to the ability of the filter to remove particles from the airstream, represented as one minus the ratio of particle concentrations measured downstream of the filter to that measured upstream of the filter. Filter testing is conducted at flow rates between 472 CFM ( $0.22 \text{ m}^3/\text{s}$ ) and 3,000 CFM ( $1.4 \text{ m}^3/\text{s}$ ) in Standard 52.2 laboratory tests. The test procedure for device efficiency uses laboratory-generated potassium chloride particles and synthetic dust to simulate field conditions.

There are two types of pressure within duct systems: static and velocity pressure. Static pressure is often simply called “pressure”. Every point in a fluid will have a static pressure, which is the force per unit area at that point. The force is equal in all directions. Velocity pressure is often called dynamic pressure. Velocity pressure is the pressure from a moving fluid when it makes a direct hit on an object, such as a register at the end of a

duct. Pressure is measured in inches of water column (IWC) or Pascals (Pa). Total system pressure is the sum of the static and velocity pressure at a given point in the HVAC system. Pressure drop refers to the pressure difference across the filter or any other component within the HVAC system's air stream (AC evaporator coil, humidifier, etc.).

Efficiency measurements for mechanical and pleated filters are performed at several intervals during a simulated dust-loading procedure in Standard 52.2 to establish a curve of efficiency as a function of dust loading. Measurements are taken at the following points:

- a. Before any dust is fed to the device;
- b. After an initial conditioning step with a dust loading of 30 g or an increase in 10 Pa (0.04 in. of water) pressure drop across the device, whichever comes first;
- c. After the dust-loading increments have achieved an airflow resistance increase of one-quarter, one-half, and three-quarters of the difference between the beginning and the prescribed end point limit of airflow resistance; and
- d. After the dust increment that loads the device to its prescribed end point resistance limit (ANSI/ASHRAE 2007).

The result of this test is the filter's Minimum Efficiency Reporting Value (MERV) rating, which is a measure of efficiency of the filter at removing particles at various size bins from 0.3 to 10  $\mu\text{m}$ . This efficiency-testing standard is also somewhat helpful for defining when a filter is "dirty." The device is assumed to be clean when the filter resistance is equal to the initial resistance value in Table 12.1 (ANSI/ASHRAE 2007). A very dirty (fully loaded) filter has resistance equal to the final resistance value, although translation to actual operational environments is difficult. A dirty filter has a resistance value in the middle of the two extremes. Beyond these inferences, there is little literature on what constitutes a dirty filter.



Low-efficiency filters are typically defined as having a MERV rating of under 4. Medium-efficiency filters have MERV ratings of 5-10 and high-efficiency filters are MERV 11 and above. Most residential HVAC filters are currently sold at 1-inch depths, although higher efficiency filters (e.g., MERV 13+) are now being sold at 2-inch and 5-inch depths, which have the benefit of providing more filter surface area for particle collection while minimizing impacts on initial filter pressure drop.

### **Coil Fouling**

Filters are used to protect HVAC equipment from damage and coil fouling and to improve indoor environmental quality for occupants. Coil fouling effects cooling capacity in two ways: by reducing the heat transfer coefficient and reducing airflow. Siegel et al. (2002) applied experimental and simulation results to estimate the impact of coil fouling on AC system performance and capacity. They found that typical coils foul enough within 7.5 years to double evaporator pressure drop. When a typical residential system coil was fouled, the pressure drop increased by about 40%, the airflow reduced 5-10%, and the efficiency and capacity of the AC decreased 2-4%. Although this is a relatively minor decrease in efficiency and capacity, this is based on assumed correct airflow. Residential systems often have low airflow and performance impacts can be greater because air conditioner capacity is more sensitive to changes in low airflows (Parker et al 1997).

Yang et al. (2004) studied the impact of different filter types on the performance of packaged air conditioners under both clean and fouled conditions. They evaluated three packaged systems: one 35-ton, one 5-ton, and one 3-ton unit. The units represent typical systems for a medium to large commercial building, small commercial building, and a small commercial or residential building, respectively. They introduced a set amount of particles to foul the coils over time and measured the percent passing through

the filter. Field measurements as well as manufacturers data was collected and integrated into a system simulation model, ACMODEL.

Somewhat surprisingly, Yang et al (2004) found that the heat transfer coefficient could actually increase with limited fouling and that under extreme fouling the coefficient reduction was minor. Capacity reduction was primarily the result of airflow reduction. After introducing the equivalent of one year's worth of dust loading (600 grams of dust), the degradation in cooling capacity from coil fouling was relatively minor: 2-4% for the 35-ton system, 2-3% for the second 35-ton system, 5-7% for the 5-ton system, and 4-5% for the 3-ton system. Depending on the AC unit size, the EER was reduced by 2-10% because of fouling.

### **Pressures within HVAC Systems**

For any fixed system, the relationship between airflow and system pressure follows a quadratic relationship, presented in Equation 1 below.

$$P = k * Q^2 \tag{1}$$

where

P = system pressure (IWC or Pa)

K = constant based on measured airflow and pressure

Q = system flow (CFM or m<sup>3</sup>/s)

Airflow within an HVAC system may be measured with a Pitot-tube traverse, flow hood, flow grid, or an anemometer. Static pressure is measured with a static pressure probe (simple Pitot-tube) and a manometer.

The static pressure drop across individual components of the HVAC system is proportional to the square of the airflow rate and a coefficient of proportionality, C. The coefficient C is constant for static system components and is based on the component's geometry. A filter's coefficient changes over time as loading changes its geometry. The evaporator's coefficient will also change as moisture condenses and fouling occurs over time. A system's total coefficient is the sum of all components connected in series with duct branches connected in parallel (Equation 2) (Stephens et al 2010).

$$C_{\text{total}} = C_{\text{return}} + C_{\text{filter}} + C_{\text{CC}} + C_{\text{HC}} + C_{\text{S1}} + \frac{C_{\text{S2}} + C_{\text{S3}}}{C_{\text{S2}} \cdot C_{\text{S3}}} \quad (2)$$

where

$C_{\text{total}}$  = coefficient of proportionality for the entire system

$C_{\text{return}}$  = coefficient of proportionality for the return duct

$C_{\text{filter}}$  = coefficient of proportionality for the filter

$C_{\text{CC}}$  = coefficient of proportionality for the cooling coil

$C_{\text{HC}}$  = coefficient of proportionality for the heating coil

$C_{\text{S1}}$  = coefficient of proportionality for the first supply duct branch

$C_{\text{S2}}$  = coefficient of proportionality for the second supply duct branch

$C_{\text{S3}}$  = coefficient of proportionality for the third supply duct branch

The power draw of an AHU fan can be described as a function of the required pressure increase across the fan and the airflow rate, as shown in Equation 3 (Stephens et al 2010).

(3)

$$W_{fan} = \frac{\Delta P_{fan} \cdot Q_{fan}}{\eta_{fan} \cdot \eta_{motor}} = \frac{C_{total} \cdot Q_{fan}^3}{\eta_{fan} \cdot \eta_{motor}} = \frac{(C_{filter} + C_{system}) \cdot Q_{fan}^3}{\eta_{fan} \cdot \eta_{motor}}$$

where

$W_{fan}$  = power draw of fan

$\Delta P_{fan}$  = required pressure increase across the fan

$Q_{fan}$  = system airflow rate

$\eta_{fan}$  = efficiency of the fan

$\eta_{motor}$  = efficiency of the fan motor

$C$  = coefficient of proportionality

In an HVAC system where the airflow rate remains constant through the use of an ECM and the motor's efficiency does not change with airflow rate, the power draw of the fan is a linear function of the filter coefficient.<sup>2</sup> In this scenario, a 5% increase in total pressure drop would cause a 5% increase in fan electric power draw. Most residential HVAC fans use PSC motors, however, which do not adjust rotational speed to maintain constant airflow rates. Thus, an increase of filter pressure drop will generally decrease the airflow rate and also decrease the fan power draw for a PSC motor (Siegel et al 2007, Stephens et al 2010).

Figure 3 represents a theoretical HVAC system without airflow controls (Stephens et al 2010). System and fan curves are used to characterize HVAC system performance based on pressure and airflow. The graph illustrates the relationship between pressure and airflow. In this example, increasing the filter pressure drop by replacing the mid-MERV filter with a high-MERV filter increases the total system pressure and decreases the airflow rate (moving the working point from A to B). The reverse effect

---

<sup>2</sup> The efficiency of many ECM fans, however, changes as a function of rotational speed.

occurs when decreasing the filter efficiency or pressure drop (moving from point A to point C). In terms of the impacts on pressure and airflow, higher-efficiency filters and loaded filters are conceptual equivalents in that they both describe ways to increase filter pressure drop.

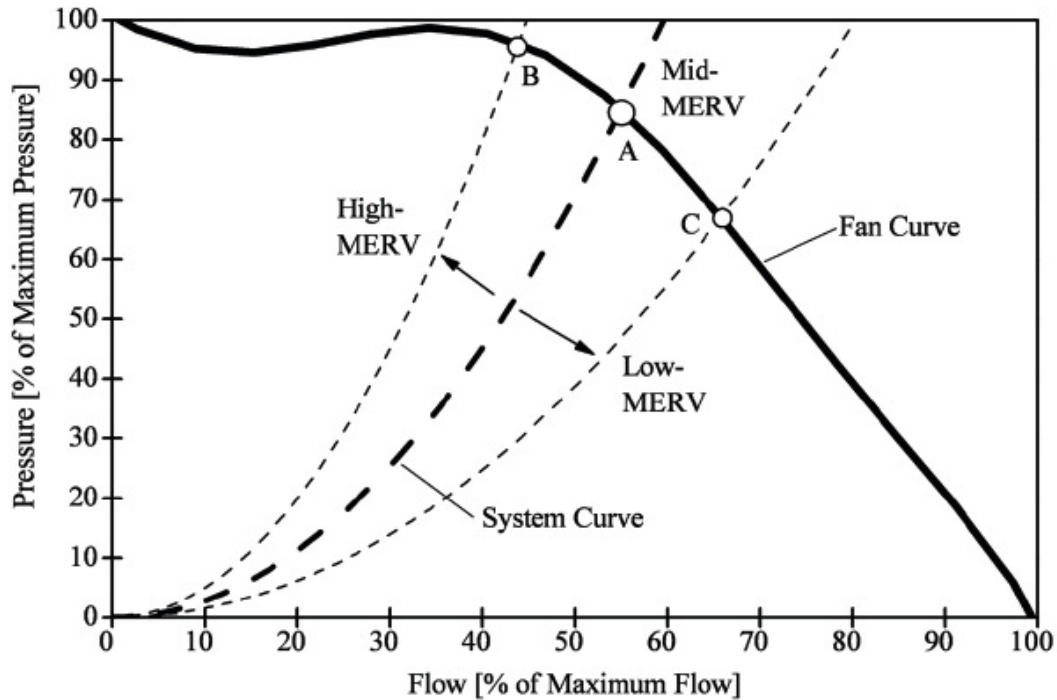


Figure 3. System and fan curves for medium-, high-, and low-pressure-drop filters (Stephens et al 2010).

However, calculating the effect of filter pressure drop on air conditioner capacity, efficiency, and overall power draw is far from straightforward. The intersection point between the fan curve and the system curve determines airflow through an air conditioner. The fan and its installation determine the fan curve. The flow resistance of all the components throughout the system, including return duct, filter, coil, and supply duct, determines the system curve. Increasing the pressure drop of the filter will have a different effect on the system curve depending on the flow resistance of the rest of the

system. To further complicate matters, residential fan curves have different slopes at different points, which means that changing the filter pressure drop of a system operating at one point in the curve will have a different effect than changing the pressure at another point on the same curve.

All filters restrict some amount of airflow. This restriction is quantified by calculating the difference in pressure immediately upstream and downstream the filter, which is known as pressure drop. One recent study in California measured filter pressure drop in 34 split air conditioners with furnaces (Proctor 2012). They found that the typical replacement filter had 0.282 in. w.c. of pressure drop. The pressure drops ranged from 0.075 to .792 in. w.c. (approximately 20 to 200 Pa). These pressure drops are higher than expected and may negatively impact HVAC system performance. The high pressure drops reduce evaporate airflow, which “lowers the total EER and the sensible EER of the machine” (Proctor 2012).

### **Airflow within HVAC Systems**

There are three common methods of measuring airflow across the evaporator coil: temperature split, balometer (airflow capture hood), and TrueFlow™ plates or an equivalent flow grid. The temperature split method was originally promoted by Carrier Corporation and allows for a quick check to establish if airflow is likely within an acceptable range (Carrier Corporation 1994). Airflow is qualitatively assessed based on the dry-bulb temperature drop across the evaporator coil and the return plenum wet-bulb temperature. First, the actual temperature split is calculated (return air dry-bulb temperature minus the supply air dry-bulb temperature). Second, using the Carrier Corporation’s table, identify the target temperature split using the return air wet-bulb temperature and return air dry-bulb temperature. And finally, calculate the difference between the target and actual temperature split (actual temperature split-target temperature split). A difference of  $\pm 3^{\circ}\text{F}$  is deemed probably acceptable while outside

that range requires further investigation.

Balometers, such as the Alnor Flow Hood and The Energy Conservatory's FlowBlaster™ Capture Hood Accessory for the Duct Blaster®, measure volumetric airflow from diffusers, grilles and registers (Figure 4). They consist of a capture device ("hood") that sits over the HVAC register to direct airflow to the fan. The fan speed is regulated based on the airflow coming out of the register.



Figure 4. The Alnor EBT Balometer. Image from <http://www.alnor-usa.com>

The TrueFlow plate is an example of a Pitot array or flow grid (The Energy Conservatory 2006). The plate is installed in the filter slot at the air handler or large return register. It uses multiple Pitot tubes to calculate an average velocity sampled over large area. With the HVAC system running, it provides a measurement of total system airflow. One advantage to the TrueFlow device is that it can provide airflow rates at the air handler when the filter is installed at the air handler.



Figure 5. TrueFlow® Air Handler Flow Meter (The Energy Conservatory, 2006).

Airflow through an HVAC system is limited to the capacity of the air handler fan. For example, an air handler fan rated for 800 CFM simply cannot move any additional air. The airflow through the system may be reduced due to undersized ducts, dirty filters, and dirty evaporator coil. Downey and Proctor (2002) evaluated airflow testing from 13,258 HVAC systems and found that 21% of the residential and commercial systems experienced low air flow across the evaporator coil. Low airflow was usually the result of “dirty filters, fouled coils, dirty blower wheels, or incorrect blower speed settings.” Reduced airflow impacts an air conditioner’s ability to cool and dehumidify air. The air conditioners total cooling capacity consists of the ability to remove latent and sensible heat. Reduced airflow reduces sensible heat transfer to the evaporator coil, which reduces sensible cooling capacity. This leads to cooler coil surface temperatures, which increases moisture removal. The reduced airflow allows longer contact time between the air and cooler coil, which improves dehumidification and latent capacity. These interactive effects result in a reduction of cooling capacity that is not directly proportional to the change in airflow, although information is lacking on in-situ measurements of these impacts in real residential environments.



## **Filters Impact on Energy Consumption**

In large commercial and high-efficiency residential systems the fan and motor controls typically maintain the required airflow rates regardless of pressure drop. These ECMs will adjust airflow rates to compensate for changes in pressure drop. For this reason, a greater pressure drop will generally lead to increased energy consumption (Chimack and Sellers 2000, Fisk et al 2002).

The Chimack and Sellers (2000) study was conducted in an office building in Hoffman Estates, Illinois with two nearly identical variable air volume (VAV) fan systems to determine if premium air filters are financially sound investments for building owners. Premium filters need to be replaced less, reducing maintenance costs, and are less restrictive to airflow. One VAV fan system, the control group, operated with standard bag-type air filters, while the second VAV operated with premium filters. Bag filters use dry media that is arranged in a long stocking shape to extend their surface area or to allow recovery of the collected material. Although bag filters are commonly used in commercial HVAC systems, many are being replaced with rigid dry filters. Power draw of the supply fan motors was monitored for 40 weeks. Static pressure drops across the filters were routinely measured, although it was impossible to isolate the pre-filter and final filters, so only a total filter system drop was recorded.

The total power draw of the system with high-MERV filters was approximately 21 percent less than the control system. The relationship of filter loading to time was nearly linear with the prefilter capturing the majority of particles. The authors do not provide the static pressure data nor did they measure airflow rates. A payback of upgrading filters was calculated at 10-months to 2 years.

Nassif (2012) explored the impact of air filtration on energy consumption for a typical air-conditioning system with a constant- or variable-speed fan. HVAC performance was modeled in eQuest, a software package that uses DOE 2.1-E hourly building energy simulation engine, combined with a direct expansion AC (ACDX)

computer model (Brandemuehl and Andersen 1993). eQuest was used to evaluate the annual energy consumption for the AC systems under a range of flow and capacity conditions. ACDX was used to model the effect of reduced airflow rate on cooling performance. A typical storefront building was modeled in each of Greensboro (NC), Orlando (FL), New York (NY), and San Francisco (CA). For constant-speed AC systems, as the filter gets dirty, the static pressure increases and the airflow rate drops. The total system cooling capacity and sensible cooling capacity both drop with lower airflow, whereas the latent cooling capacity increases. For example, the ACDX model simulated a drop to 80% of designed airflow causing a reduction in the total system capacity to 96.1% and the sensible capacity to 92.1% of design value. The annual cooling energy use was predicted to increase between 50 and 70 kWh per ton and the fan energy use increased 60-80 kWh per ton in these commercial simulations.

For variable-speed AC systems, as dirty filters increase resistance, the fan increases its speed to maintain a constant airflow and meet the sensible load requirements of the building. Since there is no change in airflow rate there is little to no direct change in cooling and heating energy use. Increased fan use generates more waste heat, which slightly increases the cooling energy use and reduces heating energy use. The increase in fan energy use ranged 15-20 kWh per ton (Nassif 2012).

Stephens et al. (2010) explored the theoretical, as well as measured, energy implications of higher-pressure drop filters. The study analyzed the energy consumption of filters in two air conditioning systems in a test house in Austin, Texas over the course of four months. The study's results are summarized in Table 1.

Table 1 Results from Stephens et al. (2010) when moving from a low-MERV filter

<b>Low-MERV Replacement</b>	<b>Airflow Change</b>	<b>Fan Power Draw</b>	<b>Outdoor Unit Power Draw</b>	<b>Total Cooling Capacity</b>
High-MERV	- 7% and 11%	+ 3-4%	- <1%	-3-4%
Mid-MERV	- 3% and 8%	+0-2%	- <1% and +<1%	-1-2% and -6-7%

Compared to low-MERV filters, high-MERV filters decreased airflow rates by approximately 7% and 11% and mid-MERV filters decreased airflow rates by approximately 3% and 8% in each of the two systems. With high-MERV filters, the fan power draw actually increased approximately 3–4% and the power draw of the outdoor unit decreased less than 1%. With mid-MERV filters, the fan power draw increased between 0%–2% and power draw of the outdoor unit decreased less than 1% in one system and increased less than 1% in the other. Total capacity and system efficiency decreased approximately 3%–4% in the presence of high-MERV filters and 1%–2% in one system and approximately 6%–7% in the other system in the presence of mid-MERV filters. The “daily energy consumption did not significantly differ between low- and high-MERV filter installations” (Stephens et al 2010).

Nassif (2012) and Stephens et al (2010) acknowledge that elevated pressures within the ductwork will increase duct leakage, but no known studies currently explore this relationship or account for this in energy calculations.

Palani et al (1992) used a standard split system air conditioner with a short-tube orifice expansion device installed within a laboratory (“bench test”) to evaluate the impact of reduced evaporator airflow on system performance. “Reduction in evaporator airflow was simulated using a plywood restriction board to cover the supply air duct. The plywood board was pre-drilled at several places to allow airflow from 100 CFM to 1000 CFM.” The study found that “at 90% reduced evaporator air flow rate, the total power consumption decreases by 17% and the EER decreases by 71%.” Reduced airflow also resulted in increased moisture removal and a reduced SHR.

Rodriguez et al (1996) also looked at the impact of reduced evaporator airflow on HVAC system performance. They tested two residential sized air conditioners in a psychrometric room. They reduced evaporator airflows between 0 and 50% below manufacturers recommendations. One unit used a TXV and the other a short tube orifice. For the TXV system, capacity and coefficient of performance (COP) actually improved with a 10% reduction in airflow, but then decreased significantly at larger airflow reductions. A 20% reduction in airflow resulted in approximately 1% drop in capacity, 2% reduction in COP, and 1% increase in power consumption. At that same reduced airflow the orifice system's capacity reduced 10%, COP dropped 8%, and power consumption increased by 1%. Capacity and COP also decreased as outdoor temperatures increased. The impact was greater on the orifice controlled system.

## CHAPTER 3

### METHODOLOGY

This section details the process for: a) selecting test homes and air conditioning equipment; b) performing measurements at different stages of simulated filtration loading; and c) data analysis. Figure 6 below outlines the research process.

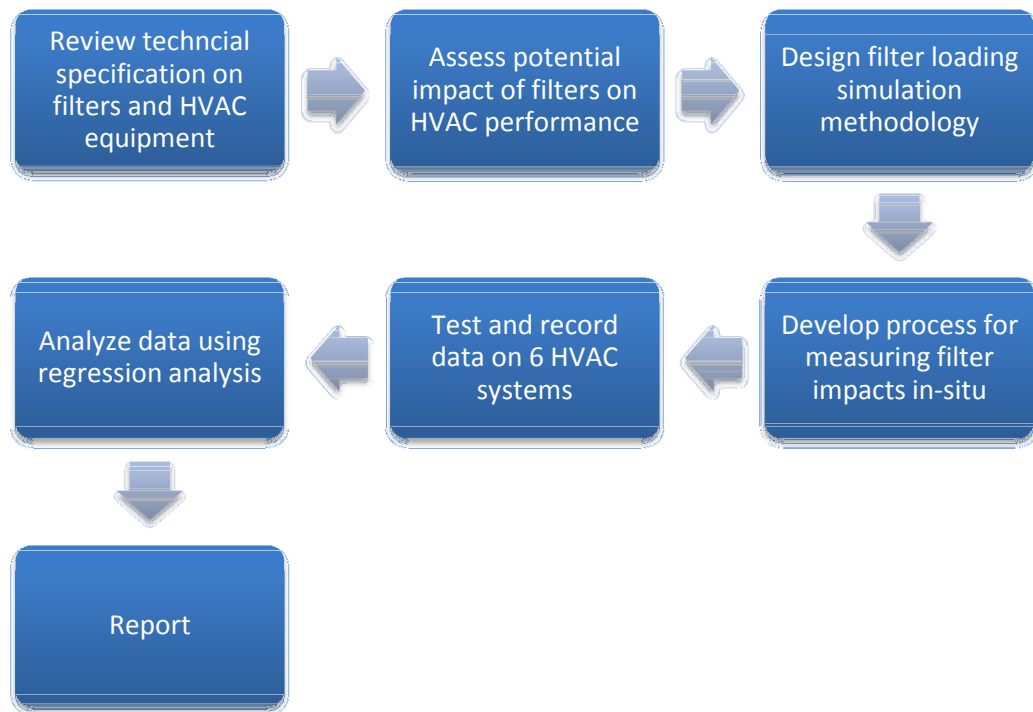


Figure 6 Research process workflow.

#### Research Design

As HVAC filters become loaded with dirt, dust, and other pollutants, the airflow through the entire duct system becomes restricted, increasing the pressure drop across the filter. This restriction of airflow causes cooling systems to run longer to provide adequate cooling if they have PSC blowers. If they have ECM blowers, system runtime should not change drastically for most loading conditions, although the fan will draw more power to overcome the additional pressure drop. Therefore, any energy savings from filter

replacement depends on the extent of filter loading (i.e., filter pressure drop) and fan blower type, either permanent split-capacitor (PSC) or electronically commutated motors (ECM). This study documents the impact of simulated filter loading in-situ on a small, but generally representative, sample of Atlanta area homes.

### Test House Selection

This pilot study assessed homes within the Atlanta metro-region. Since the 1970s, the Atlanta region has experienced remarkable growth with a sustained influx of new residents. According to the Atlanta Regional Commission (ARC) nearly 80% of all homes have been built since 1970 (ARC unknown). Although the exact number of homes with central air conditioning in the metro-region is unknown, for decades the majority of new homes have been built with AC (U.S. Census Bureau 2009). Figure 7 below shows the growth of air conditioning in the south.

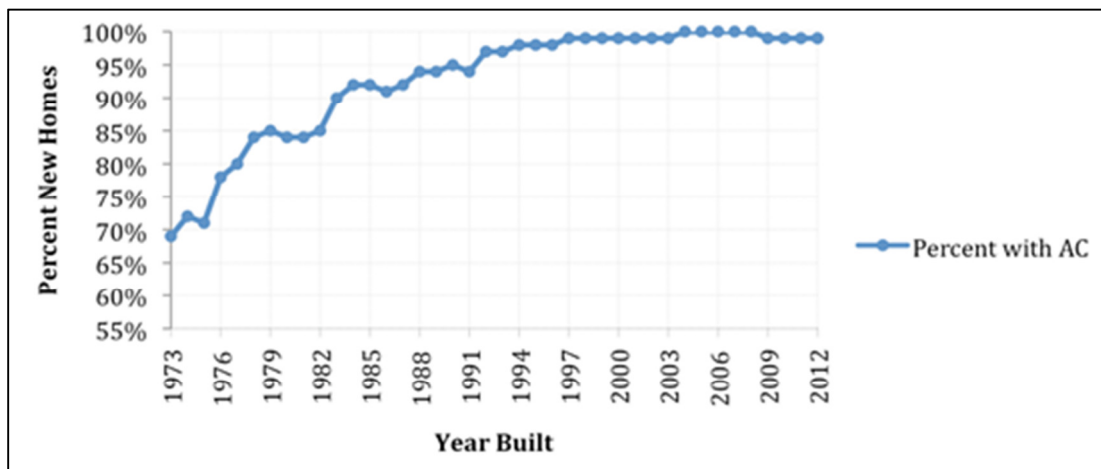


Figure 7. Percent of new homes containing central air conditioners in the south region (U.S. Census Bureau 2009).

Four homes within the Atlanta metro-region were selected for testing. The homes all contain central forced-air AC or air source heat pump systems located in

unconditioned spaces such as basements, attics, or crawlspaces. HVAC systems in the Southeast US are commonly located within unconditioned spaces. The selected homes ranged in age from nearly 90 years old to approximately 65 years old, and the HVAC systems were between 1 and 10 years old. The HVAC systems ranged from 2 to 4 tons. They include Rheem, Trane, Ruud, and Carrier brand equipment. Lance Beaton with VIS VIVA Energy Consulting, an Atlanta based home performance and HVAC contracting company, confirmed that these brands represent some of the most common HVAC systems sold in the Atlanta area (Beaton 2013). Thus the HVAC systems were considered representative of those installed in Atlanta homes over the past 10 years.

A total of 5 AC systems were assessed for this initial phase of testing. Four homes had one system each and one home had two systems. Tested systems were selected to include both horizontal and vertical configurations. All systems had filters located at the air handling unit (AHU). A range of filter sizes was included. The testing methodology compares the HVAC system “as-is” to induced, or simulated, loading conditions. The as-is conditions serve as the baseline to measure the impact of filter loading. Because our testing included only the HVAC system itself and not its ability to cool any particular space, housing characteristics such as building structure, thermal envelope, shading from sunlight did not impact the testing methodology. Table 2 summarizes the test system characteristics.

Table 2. Test system characteristics

Test System	Home Characteristics		HVAC Characteristics		
	Year Built	Size (ft <sup>2</sup> )	Year Manufactured	Size (tons)	Location
1	1950s	1,700	2009	2.5	Vented Crawlspace
2	1939	2,014	2012	2.5	Unconditioned Basement
3	1939	2,014	2012	2	Attic
4	1927	1,750	Approx. 2003	3.5	Unconditioned Basement
5 (5- Right)	1950s	1,850	2007	4	Unconditioned Basement
6 (5-Left)	1950s	1,850	2007	4	Unconditioned Basement

### ***Filter Loading Simulation***

This study simulated filter loading by installing the TrueFlow airflow metering device and partially taping off the face at 3 different increments, similar to the procedure in Palani et al. (1992). This resulted in measurements at five discrete static pressures and simulated loading conditions: no filter, TrueFlow measurement, TrueFlow Taped #1, TrueFlow Taped #2, and TrueFlow Taped #3. Examples of the TrueFlow taped for the three consecutive measurements are below (Figures 8 - 10). The exact amount and placement of the tape varied between homes to take into account the measured performance of individual HVAC systems. The TrueFlow was not used to measure airflow once taped.





Figure 8 An example of a partially taped filter (“TrueFlow Taped 1”)



Figure 9. An example of a partially taped filter (“TrueFlow Taped 2”).



Figure 10. An example of a partially taped filter (“TrueFlow Taped 3”).

### **Data Collection**

The following information about each HVAC system was collected and measured: AC indoor and outdoor coil make and model numbers, furnace (if present) make and model number, and presence of mechanical ventilation. Testing was performed during periods when the outdoor temperature was above 60°F to allow for the safe operation of air conditioners.

Measurements were taken after the HVAC system reached approximately steady state. Steady State refers to the point at which the system is running at peak efficiency and the evaporator coil is fully cooled. Since AC units cycle on and off as they maintain their desired temperature, it is important to properly identify steady state. Steady state was identified based on a constant difference of air characteristics (pressure, temperature, and relative humidity) across the coil. Palani et al (1992) found that the test bench

reached steady state within 4 minutes after switching on the unit. Measurements in this work were taken after at least 10 minutes of operation, once steady state was achieved. Measurements were recorded with the filter removed, TrueFlow installed, and the TrueFlow partially taped at three different intervals.

Three HVAC system configurations were tested. Figure 11 below shows a vertical HVAC system with one central filter. Figure 12 is a horizontal HVAC system with one central filter.

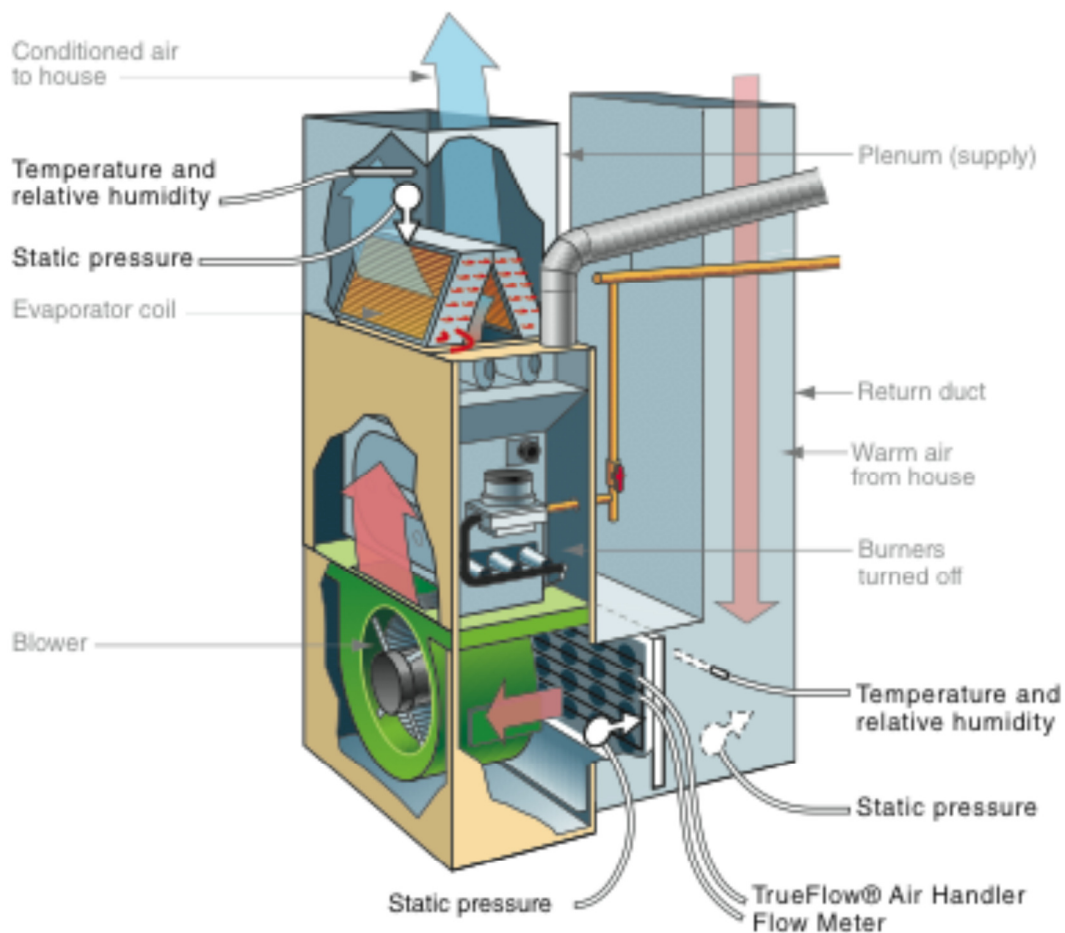


Figure 11. Vertical HVAC system with one central filter. Image courtesy Terrel Broiles.

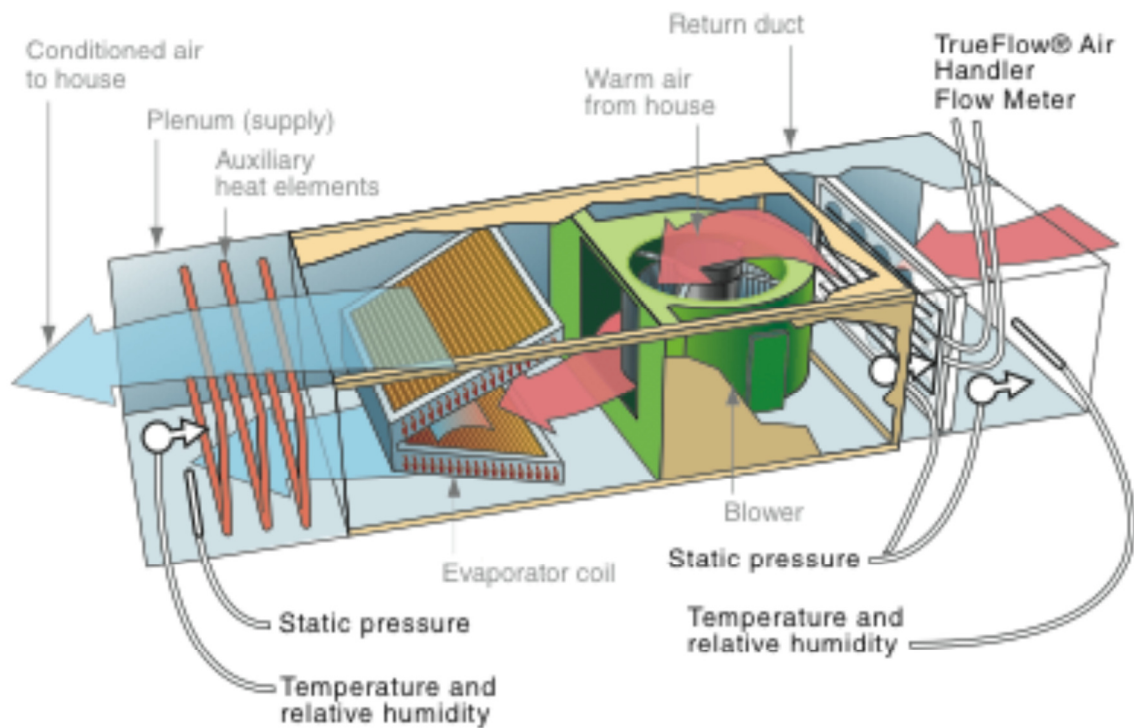


Figure 12. Horizontal HVAC system with one central filter. Image courtesy Terrel Broiles.

The Figure 13 below shows the vertical HVAC system with two return plenums each with a central filter. The return plenums were tested independently. This figure shows the set up for testing the left side only.

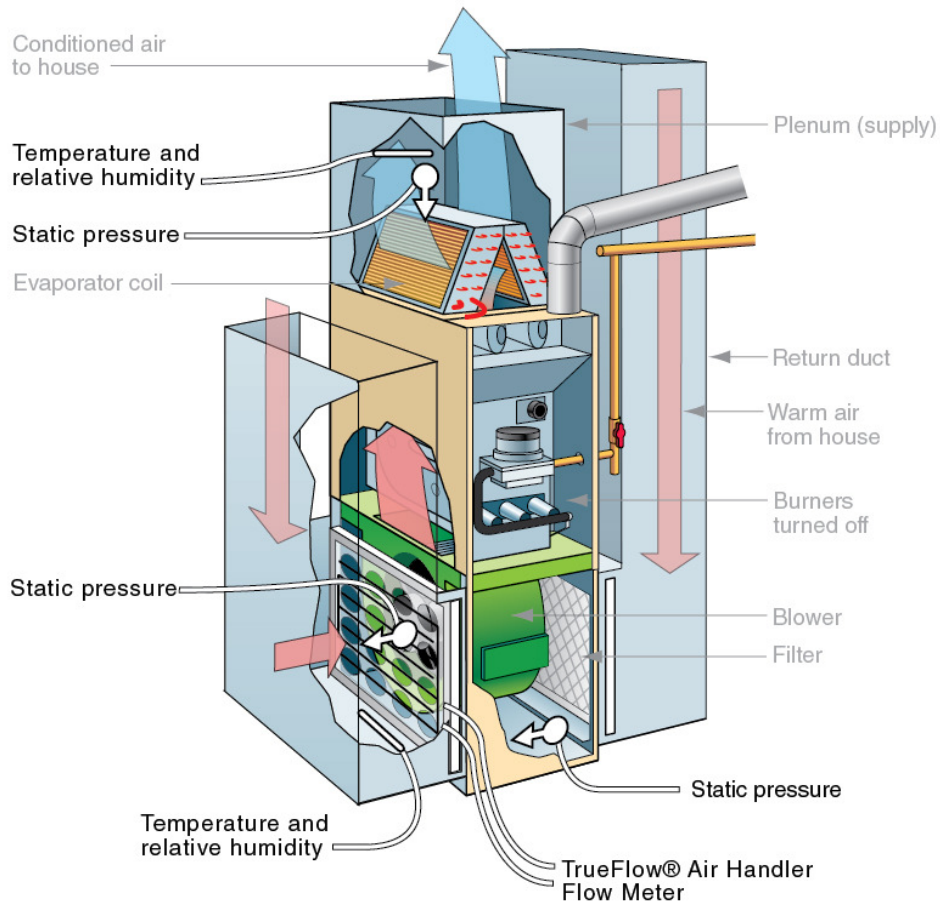


Figure 13. Vertical HVAC system with two central filters. Each side of the system was tested independently. This shows the configuration to test the left side. Image courtesy Terrel Broiles.

### Fan Curve Determination Procedure

A series of measurements were first conducted to establish fan curves and to better understand the relationship between airflow and filter pressure drop in the test systems. Measurements were recorded within the supply plenum, return plenum, and between the evaporator coil and filter. The measurements include static pressure before and after the filter; static pressure before and after the evaporator coil; temperature before and after the evaporator coil; and relative humidity before and after the evaporator coil.

Table 3 below summarizes the location and type of measurements recorded.



Table 3. Measurement type and location

Measurement Location	Measurements Recorded
Return plenum	Dry-bulb temperature (°C), relative humidity, and static pressure (Pa)
Supply plenum	Dry-bulb temperature (°C), relative humidity, and static pressure (Pa)
Coil side of filter	Static pressure (Pa)

The testing equipment is presented below in Table 4.

Table 4. Testing instrumentation

Measurement	Units	Equipment	Accuracy
Pressure	Pa (IWC)	Energy Conservatory DG-700	± 1% of reading or 0.15 Pa (0.0006 IWC)
Temperature	°C (°F)	Fieldpiece ARH4	±1°F for readings 32°F to 113°F
Relative Humidity	%RH	Fieldpiece ARH4	±2.5% @ 77°F(25°C), 10% to 90% RH
Airflow	m3/h (cfm)	Energy Conservatory TrueFlow Plate	±7% of reading

The filter face was partially sealed with tape to restrict overflow, simulating filter loading and higher MERV equipment. Airflow rates were calculated in the field using Trueflow and the measured supply pressure. System measurements were required with the filter removed, TrueFlow installed, and the TrueFlow partially sealed at 3 intervals to achieve a total airflow reduction of 40%. Since there is no known research using tape to simulate filter loading, this process was carefully evaluated and documented.

The TrueFlow Manual provides equations for estimating adjusted airflow (Equation 4) based on measured supply plenum pressure (The Energy Conservatory 2006).

$$Qf_{an} = Q_{reference} \sqrt{\frac{\Delta P_{operating}}{\Delta P_{reference}}} \quad (4)$$

where

$Q_{reference}$  = volumetric flow rate of air with measuring device installed, m3/h (cfm)

$\Delta_{\text{Preference}}$  = supply plenum pressure with measuring device installed, Pa (in. w.c.)

$\Delta_{\text{Poperating}}$  = operating supply plenum pressure, Pa (in. w.c.)

Sensible, latent, and total capacity will be calculated for each of the 5 system

conditions based on the following equations used by Stephens et al. (2010). The sensible

capacity,  $q_{\text{sensible}}$  (kW, kBtu/hr), is calculated using the Equation 5.

$$q_{\text{sensible}} = Q_{\text{fan}} \rho (C_p \Delta T) \quad (5)$$

where

$Q_{\text{fan}}$  = volumetric flow rate of air flowing through the cooling coil, m<sup>3</sup>/s (ft<sup>3</sup>/hr)

$\rho$  = air density, assumed constant, 1.2 kg/m<sup>3</sup> (0.075 lbm/ft<sup>3</sup>)

$C_p$  = specific heat of air, assumed constant, 1.005 kJ/(kgK), (0.24 Btu/[lbm°F])

$\Delta T$  = temperature difference across the cooling coil, K (°F)

The latent capacity,  $q_{\text{latent}}$  (kW, kBtu/hr), is calculated using Equation 6.

$$q_{\text{latent}} = Q_{\text{fan}} \rho (W h_{fg}) \quad (6)$$

where

$Q_{\text{fan}}$  = volumetric flow rate of air flowing through the cooling coil, m<sup>3</sup>/s (ft<sup>3</sup>/hr)

$\rho$  = air density, assumed constant, 1.2 kg/m<sup>3</sup> (0.075 lbm/ft<sup>3</sup>)

$\Delta W$  = humidity ratio difference across the cooling coil, kg/kg (lbm/lbm)

$h_{fg}$  = latent heat of vaporization for water, assumed constant, 2257 kJ/kg (970 Btu/lb)

The total capacity,  $q_{\text{total}}$  (kW, kBtu/hr), is the sum of the sensible capacity

(Equation 5) and latent capacity (Equation 6). Total capacity is expressed in Equation 7.

$$q_{\text{total}} = Q_{\text{fan}} \rho (C_p \Delta T + W h_{fg}) \quad (7)$$

where

$Q_{\text{fan}}$  = volumetric flow rate of air flowing through the cooling coil, m<sup>3</sup>/s (ft<sup>3</sup>/h)

$\rho$  = air density, assumed constant, 1.2 kg/m<sup>3</sup> (0.075 lbm/ft<sup>3</sup>)

$C$  = specific heat of air, assumed constant, 1.005 kJ/(kgK), (0.24 Btu/[lbm°F])

$\Delta T$  = temperature difference across the cooling coil, K (°F)

$\Delta W$  = humidity ratio difference across the cooling coil, kg/kg (lbm/lbm)

$h_{fg}$  = latent heat of vaporization for water, assumed constant, 2257 kJ/kg (970 Btu/lb)

## Data Analysis

The data was analyzed to assess the relationship between filter pressure drop and airflow rates; filter pressure drop and temperature differences across the coil ( $\Delta T$ ); filter pressure drop and absolute humidity differences across the coil ( $\Delta W$ ); airflow rate and temperature differences across the coil ( $\Delta T$ ); and airflow rate and absolute humidity differences across the coil ( $\Delta W$ ). Finally, the relationship between airflow rate and sensible, latent, and total capacities were also evaluated. Regression analysis was used to determine the strength of each relationship. The results from simulated filter loading were also compared to previous studies to estimate the impact of reduced airflow rates on air-conditioner energy consumption.

Finally, because the nature of data collection in the field can result in periodic improper measurements, a method of calculating an observation's Z-score was used to identify whether or not an observation was a statistical outlier in the dataset. A Z-Score is a statistical measurement of an observation's relationship to the mean in a group of scores. The z-score calculation is below in Equation 8.

$$Z_i = \frac{Y_i - \bar{Y}}{s} \quad (8)$$

where

$Y_i$  = sample value

$\bar{Y}$  = sample mean

$s$  = standard deviation

A Z-score of 0 means the score is the same as the mean. The Z-score can also be positive or negative, indicating whether it is above or below the mean and by how many standard deviations. A Z-score of 3.5 means the observation is at least 3.5 standard deviations from the mean, which serves as a common criterion for identifying outliers in



datasets like this one. The Z-score analysis was eventually used to remove one outlier within the data set (see pages 44-55 for additional information).

## **CHAPTER 4**

### **FIELD RESULTS & DATA ANALYSIS**

#### **Test System Descriptions**

Field testing was performed in July, August, and September 2013. Ambient air temperature ranged from approximately 64°F to 86°F during the test periods. Twenty initial test systems were excluded from analysis for not meeting key criteria. Cause for exclusion included the following: system contained a known electrically commutated motor (ECM) blower; not enough room to install measurement equipment on either side of the filter; and filter located at a central return register and not at the air handler. Four out of the six chosen test systems were known permanent split capacitor (PSC) blowers; information could not be found for test systems 5 and 6, but from the subsequent airflow and pressure data suggest that they were likely ECM blowers or at least variable speed blowers.

#### **Test System Locations**

Four houses within the Atlanta metro-region were selected for testing (Figure 14). The homes all contain central forced-air AC and/or air source heat pump systems located in unconditioned spaces (unconditioned basement, attic, or crawlspace). The houses ranged in age from nearly 65 to approximately 90 years old, and the HVAC systems ranged from 1 to 10 years old. The HVAC systems ranged from 2 to 4 tons. They include Rheem, Trane, Ruud, and Carrier brand equipment, which represent some of the most common HVAC systems sold in the Atlanta area (Beaton 2013). Thus the HVAC systems were considered generally representative of those installed in Atlanta homes over the past 10 years.

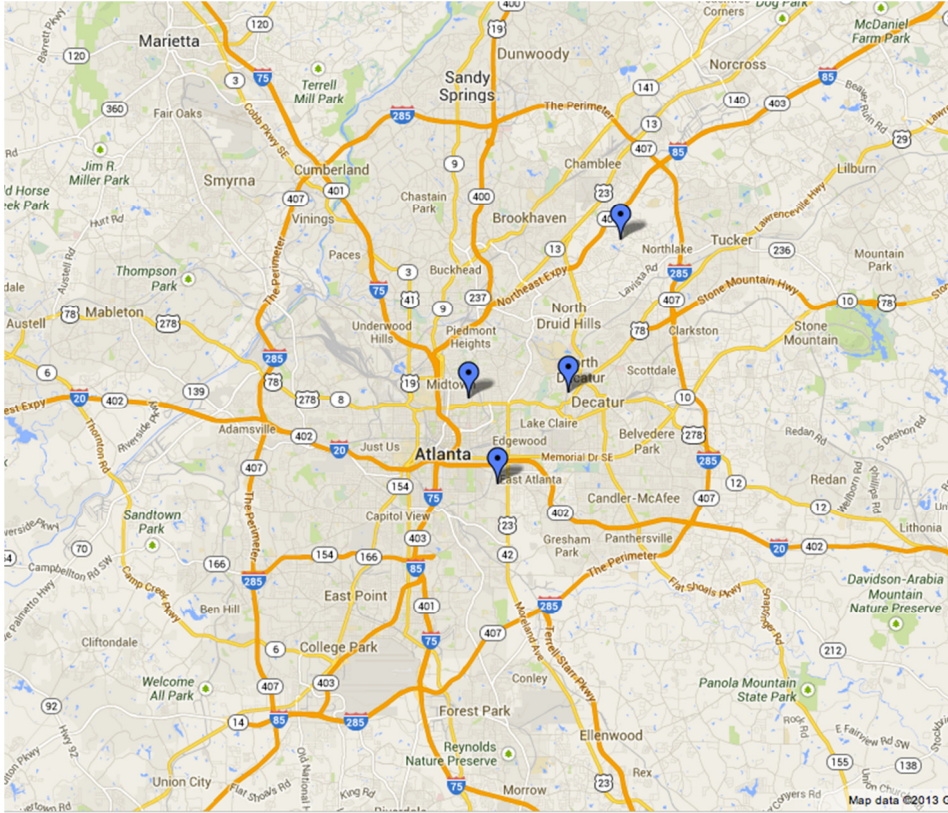


Figure 14 Location of the 4 test homes in the Atlanta metro-region.

A total of five AC systems were assessed for this initial phase of testing. Two of the systems were located within the same home. HVAC systems included both vertical and horizontal configurations. All systems had filters located at the air handler. A range of common filter sizes was included, from 14" x 20" to 20" x 24".

## Test System 1

Test system 1 is located in an unconditioned crawlspace. The house was built in the 1950s and has an area of approximately 1,700 ft<sup>2</sup>. The 2.5-ton capacity system is horizontally configured (Figure 15).



Figure 15 Test system 1 is located in an unconditioned crawlspace and is horizontally configured. The return plenum is on the right and supply plenum to the left.

## **Test System 2**

Test system 2 has a 2.5-ton capacity and is located in the unconditioned basement of a home built in 1939 (Figure 16). The home has an area of 2,014 ft<sup>2</sup>. The system was installed in 2012.



Figure 16 Test system 2 is vertically configured and located in an unconditioned basement. The return plenum is on the bottom and supply plenum above.

### **Test System 3**

Test system 3 has a 2-ton capacity and is located in the unconditioned attic of the same home as test system 2. The system is configured horizontally and was installed in 2012.

### **Test System 4**

Test system 4 has 3.5-ton capacity and is located in an unconditioned basement (Figure 17). The home was built in 1927 and is approximately 1,750 ft<sup>2</sup>. The system was installed in approximately 2003.





Figure 17 Test system 4 is vertically configured and located in an unconditioned basement. The return plenum is on the left side and supply plenum above.

### **Test Systems 5 and 6**

Test systems 5 and 6 are actually the same HVAC system. Figure 18 below shows how the system has two return plenums. Each plenum has its own filter and was tested separately. The system has 4-ton capacity, located in an unconditioned basement, and was installed in 2007. The house is approximately 1,850 ft<sup>2</sup> and built in the 1950s.



Figure 18 Test systems 5 and 6. The photo shows the left side return plenum set up for testing.

## **Analysis**

The following sections describe measured impacts of (i) filter pressure drop on system airflow rates, (ii) airflow rate reductions on temperature and absolute humidity differences across the coils, and (iii) airflow rate reductions on sensible and latent cooling capacity.

### **Filter Pressure Drop & System Airflow**

The relationship between induced filter pressure drop and system airflow rates was first evaluated in each system, as shown in Figure 19 and Table 5. The absolute value of the pressure drop across the filter was compared to the reduction in airflow (as a

percentage of total system flow without filter installed) for each induced pressure drop condition. The induced filter pressure drop ranged from 16 Pa to 231 Pa. At least 75 Pa was achieved in each system, although systems 2 and 3 did not reach 100 Pa at their maximum level of filter blockage (which was nearly 75% blocked). Airflow rates ranged from 100% of total system airflow (i.e. airflow remained unchanged) to as low as 61% (i.e., a 39% reduction in airflow at the largest filter pressure drop of 231 Pa). Overall, as filter pressure drop increased, airflow rates generally decreased, particularly for the known PSC blowers. The two systems that were apparently ECM blowers responded to increased filter pressure drop by nearly maintaining airflow rates until reaching a maximum pressure and rapidly decreasing in flow, which is consistent with other ECM data (Murray 2012).

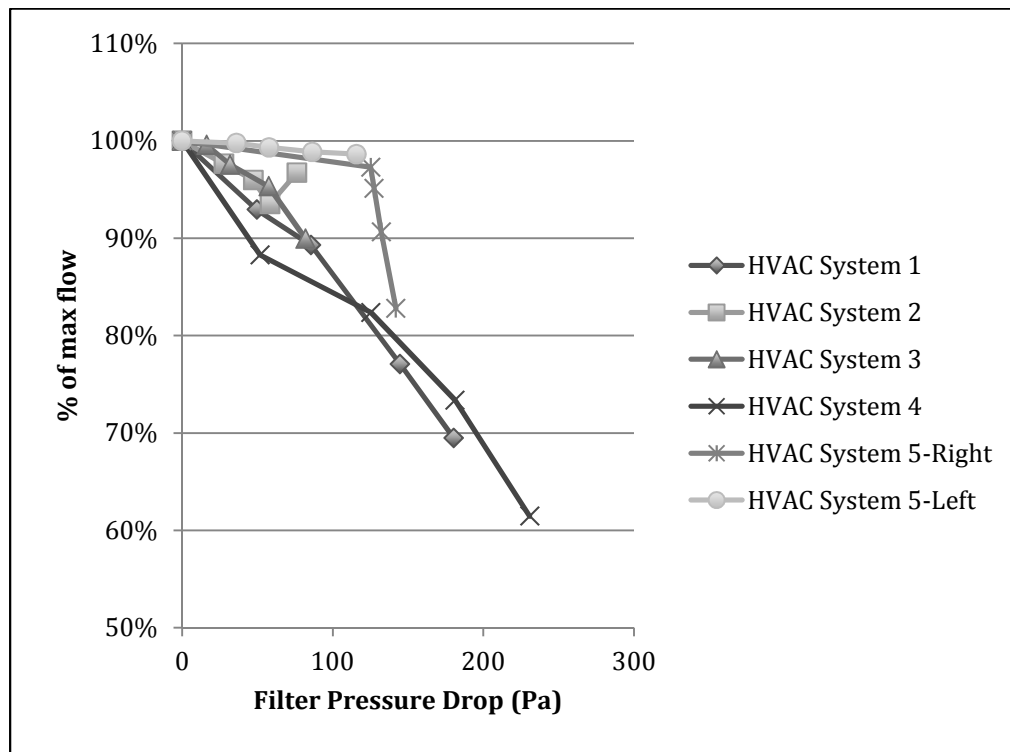


Figure 19 Relationship of induced filter pressure drop and system airflow rate measured in the test systems.



Similarly, Figure 20 shows the same airflow and filter pressure data measured at each site and simulated loading condition, combined across all data points and fit with a linear regression. Regression analysis shows an intercept near 1.02, a slope of -0.0014, and a coefficient of determination ( $R^2$ ) of 0.71, suggesting that with reasonable certainty, each additional 10 Pa in filter pressure drop resulted in a ~1.4% decrease in system airflow rates in these systems.

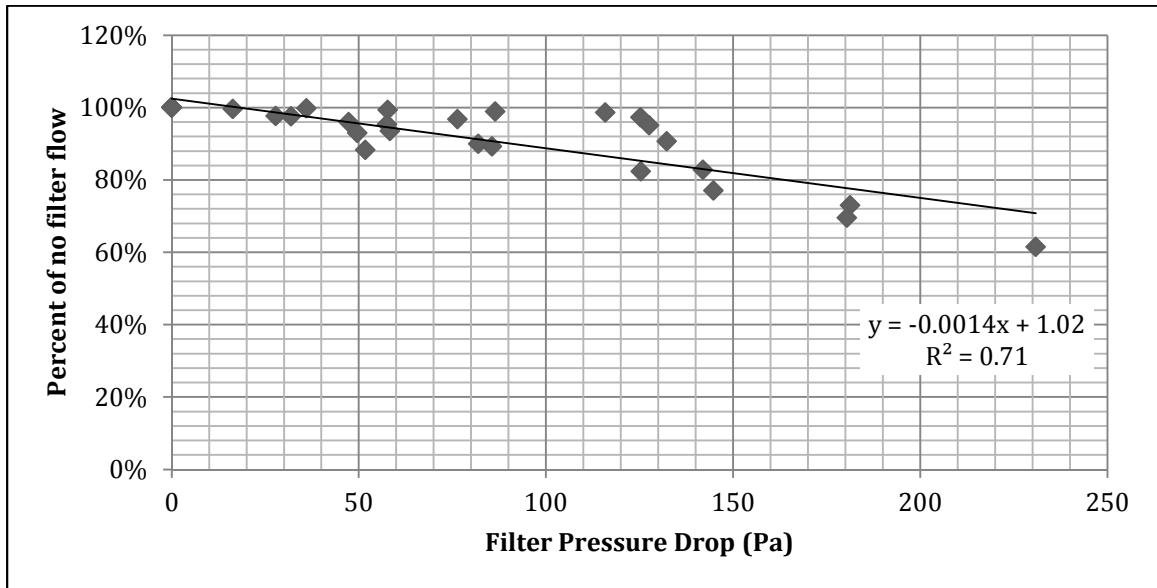


Figure 20 System airflow rates normalized to no filter conditions versus filter pressure drop.

Table 5 Filter pressure drop and system airflow

HVAC System Name	Filter pressure drop (Pa)					Percent of no filter flow (%)				
	No Filter	True Flow	True Flow Taped 1	True Flow Taped 2	True Flow Taped 3	No Filter	True Flow	True Flow Taped 1	True Flow Taped 2	True Flow Taped 3
1	0	49.6	85.6	144.7	180.4	100%	93%	89%	77%	69%
2	0	27.8	47.3	58.3	76.3	100%	98%	96%	94%	97%
3	0	16.3	31.9	57.5	81.9	100%	100%	98%	95%	90%
4	0	51.7	125.3	181.2	230.8	100%	88%	82%	73%	61%
5 (Right)	0	125.2	127.5	132.2	141.9	100%	97%	95%	91%	83%
6 (5-Left)	0	36.0	57.7	86.4	115.8	100%	100%	99%	99%	99%

Test Systems 5 and 6 could not be verified as having an ECM blower, although evidence suggests that they were at least variable speed blowers. These two systems responded to increased filter pressure drop by nearly maintaining airflow rates until reaching a maximum pressure and rapidly decreasing in flow. System 5 (left return plenum) maintained a nearly identical airflow rates regardless of filter pressure drop, at least until ~115 Pa. System 6 (right plenum of system 5) maintained airflow rates within 90% of the no filter flow until rapidly decreasing above 125 Pa.

### Filter Pressure Drop & Temperature Difference Across the Coil

The relationship between induced filter pressure drop and the dry bulb temperature difference across the evaporator coil ( $\Delta T$ ) was evaluated in each system, as shown in Table 6. The difference in temperature ( $\Delta T$ ) before passing the evaporator coil (before-filter) and after passing the coil (in the supply plenum) was measured. Values of  $\Delta T$  at each flow and pressure drop condition were normalized to those measured with no filter installed and compared to the absolute value of the pressure drop across the filter. The change in  $\Delta T$  ranged from 152% of total system airflow (i.e. the difference in temperature increased) to 97% (i.e., a 3% reduction in  $\Delta T$ ).

Table 6 Filter pressure drop and coil  $\Delta T$

HVAC System Name	Pfilt (Pa)					Percent of no filter $\Delta T$ (%)				
	No Filter	True Flow	True Flow Taped 1	True Flow Taped 2	True Flow Taped 3	No Filter	True Flow	True Flow Taped 1	True Flow Taped 2	True Flow Taped 3
1	0	49.6	85.6	144.7	180.4	100%	94%	100%	108%	123%
2	0	27.8	47.3	58.3	76.3	100%	102%	107%	107%	110%
3	0	16.3	31.9	57.5	81.9	100%	108%	110%	113%	113%
4	0	51.7	125.3	181.2	230.8	100%	102%	111%	152%*	138%
5 (5-Right)	0	125.2	127.5	132.2	141.9	100%	97%	98%	98%	97%
6 (5-Left)	0	36.0	57.7	86.4	115.8	100%	107%	109%	111%	114%

\* Data point is statistically an outlier and removed from analysis.

Importantly, the maximum change in  $\Delta T$  (System 4 with 181.2 Pa filter pressure drop) was identified visually to be a likely outlier in the dataset. To determine whether or not this was the case, a Z-score was calculated for each of the 30 data points for the relative change in  $\Delta T$  across all systems, as shown here in Equation 9:

$$Z_i = \frac{Y_i - \bar{Y}}{s} \quad (9)$$

where

$Y_i$  = sample value

$\bar{Y}$  = sample mean

$s$  = standard deviation of the sample

Z-scores for each data point are shown in Table 7 on the next page.

Table 7 Z-scores for each  $\Delta T$  measurement

Filter pressure drop (Pa)	Percent of no filter $\Delta T$ (%)	Z-score
0	100%	-0.62
0	100%	-0.62
0	100%	-0.62
0	100%	-0.62
0	100%	-0.62
0	100%	-0.62
49.6	94%	-1.14
27.8	102%	-0.47
16.3	108%	-0.01
51.7	102%	-0.42
125.2	97%	-0.89
36.0	107%	-0.09
85.6	100%	-0.62
47.3	107%	-0.03
31.9	110%	0.19
125.3	111%	0.28
127.5	98%	-0.80
57.7	109%	0.09
144.7	108%	0.06
58.3	107%	-0.03
57.5	113%	0.46
<b>181.2</b>	<b>152%</b>	<b>3.60</b>
132.2	98%	-0.80
86.4	111%	0.27
180.4	123%	1.26
76.3	110%	0.19
81.9	113%	0.46
230.8	138%	2.49
141.9	97%	-0.89
115.8	114%	0.54

The apparent outlier measured during the TrueFlow Taped 2 condition at System 4 was shown to have a Z-score of 3.6, suggesting it was indeed an outlier with a score greater than commonly used criteria of  $Z = 3.5$ . Therefore, this data point is removed from further analysis. The remaining maximum change in  $\Delta T$  is therefore 138% (at the highest filter pressure drop measured). The exact cause for the outlying data is unknown, but it was likely caused by experimental error in the field. No combination of airflow and pressure measurements was removed, however, because there were no outliers with Z-scores greater than 3.5.

Figure 21 shows the remaining relative  $\Delta T$  data versus absolute filter pressure drop measured in each of the test systems.

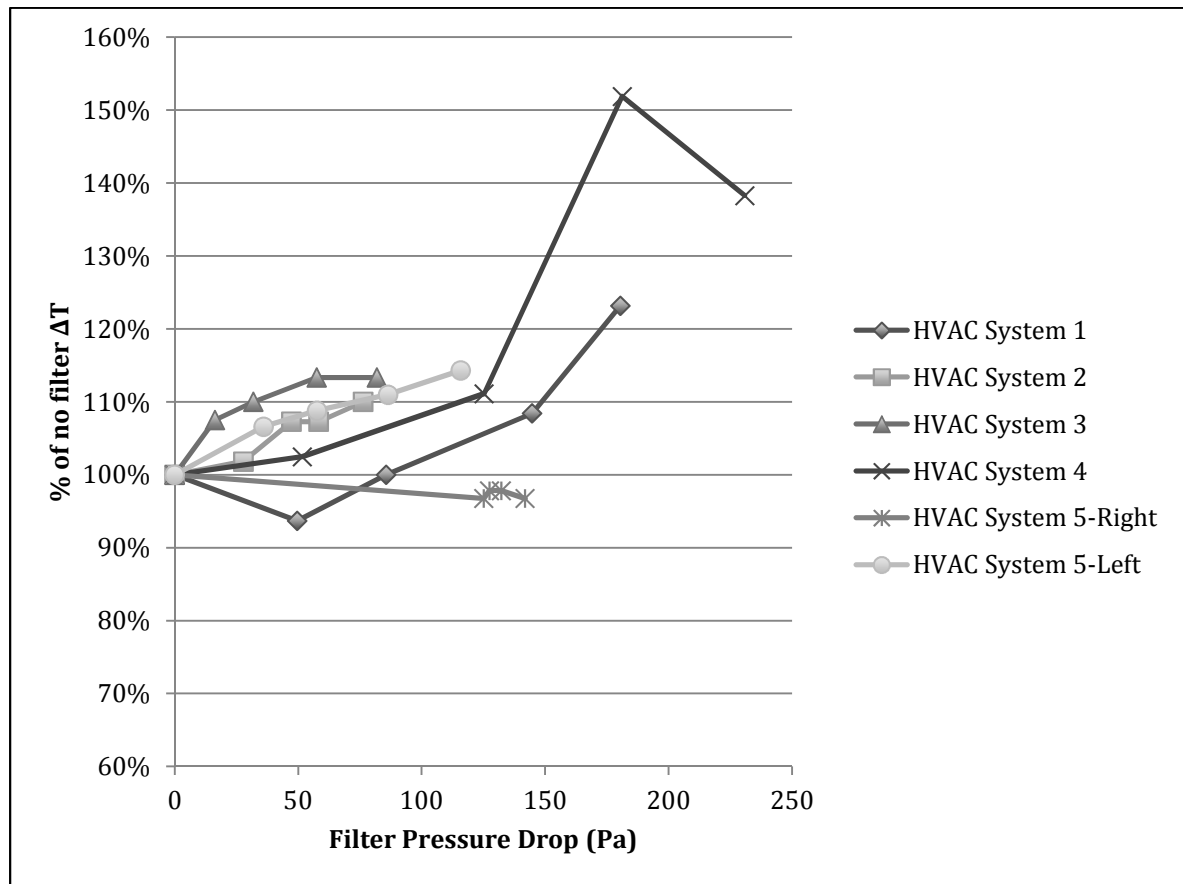


Figure 21 Relative  $\Delta T$  across the coil versus filter pressure drop for each test system.

Similarly, Figure 22 shows the same  $\Delta T$  and filter pressure drop data measured at each site and induced loading condition, combined across all data points and fitted with a linear regression. Regression analysis shows an intercept near 1.00, a slope of +0.0008 with a coefficient of determination ( $R^2$ ) of 0.30, suggesting that with only moderate certainty, each additional 10 Pa in filter pressure drop resulted in a ~0.8% increase in system  $\Delta T$  in these systems. Similarly, if filter pressure drop reaches 200 Pa, coil  $\Delta T$  is expected to increase by approximately 16% in these test systems, on average.

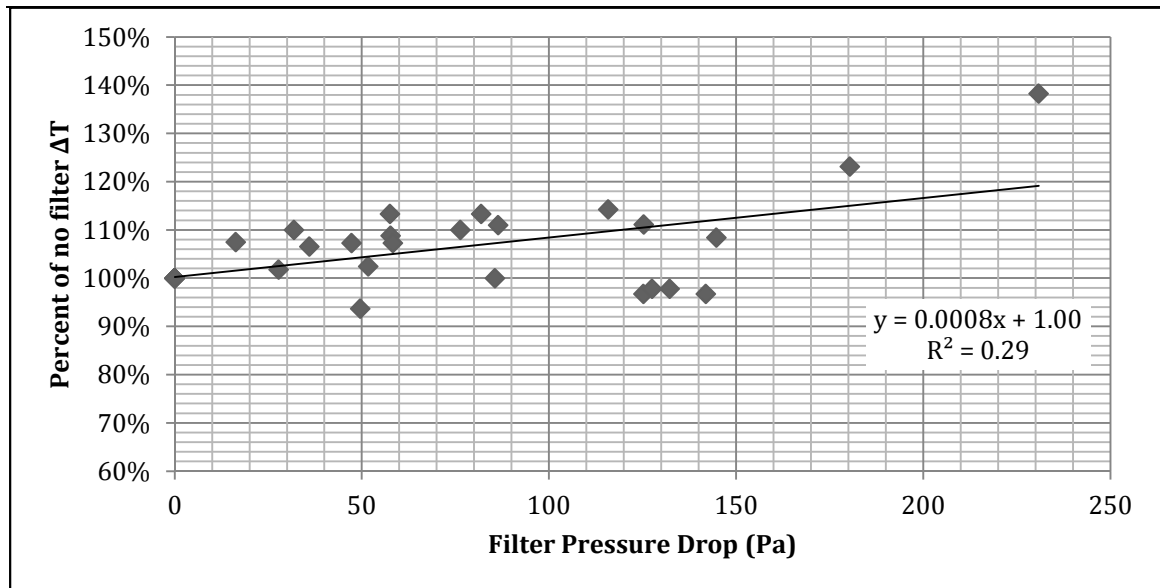


Figure 22 Relationship of filter pressure drop and  $\Delta T$  across all systems.

These data suggest what other laboratory and field studies have shown: as airflow rates are reduced in the presence of larger filter pressure drops, sensible capacity will not decrease linearly with flow because the temperature difference across the coil increases slightly and supply air is delivered at a lower temperature (Nassif 2012, Yang et al 2004). This relationship is explored further in a subsequent section.

### Filter Pressure Drop & Absolute Humidity

The relationship between induced filter pressure drop and changes in the difference in absolute humidity across the coil ( $\Delta W$ ) was evaluated in each system, as shown in Table 7. The change in  $\Delta W$  across the coil (as a percentage of  $\Delta W$  without filter installed) was compared to the absolute value of the pressure drop across the filter for each induced pressure drop condition. Because  $\Delta W$  was calculated using the dry bulb temperature and relative humidity measurements in each location, data from True Flow Taped 2 in System 4 was again excluded as an outlier. The resulting changes in  $\Delta W$

ranged from a minimum of 41% (i.e., a 59% reduction in  $\Delta W$ ) to a maximum of 100% (i.e.  $\Delta W$  did not change). These data are shown in Figure 23 for each test system.

Table 8 Filter pressure drop and absolute humidity differences across the coil

HVAC System Name	Pfilt (Pa)					Percent of no filter $\Delta W$ (%)				
	No Filter	True Flow	True Flow Taped 1	True Flow Taped 2	True Flow Taped 3	No Filter	True Flow	True Flow Taped 1	True Flow Taped 2	True Flow Taped 3
1	0	49.6	85.6	144.7	180.4	100%	41%	48%	82%	98%
2	0	27.8	47.3	58.3	76.3	100%	82%	68%	77%	82%
3	0	16.3	31.9	57.5	81.9	100%	84%	81%	81%	71%
4	0	51.7	125.3	181.2	230.8	100%	86%	77%	132%*	100%
5 (Right)	0	125.2	127.5	132.2	141.9	100%	81%	86%	95%	90%
6 (5-Left)	0	36.0	57.7	86.4	115.8	100%	100%	100%	100%	100%

\*This data point is statistically an outlier and removed from analysis.

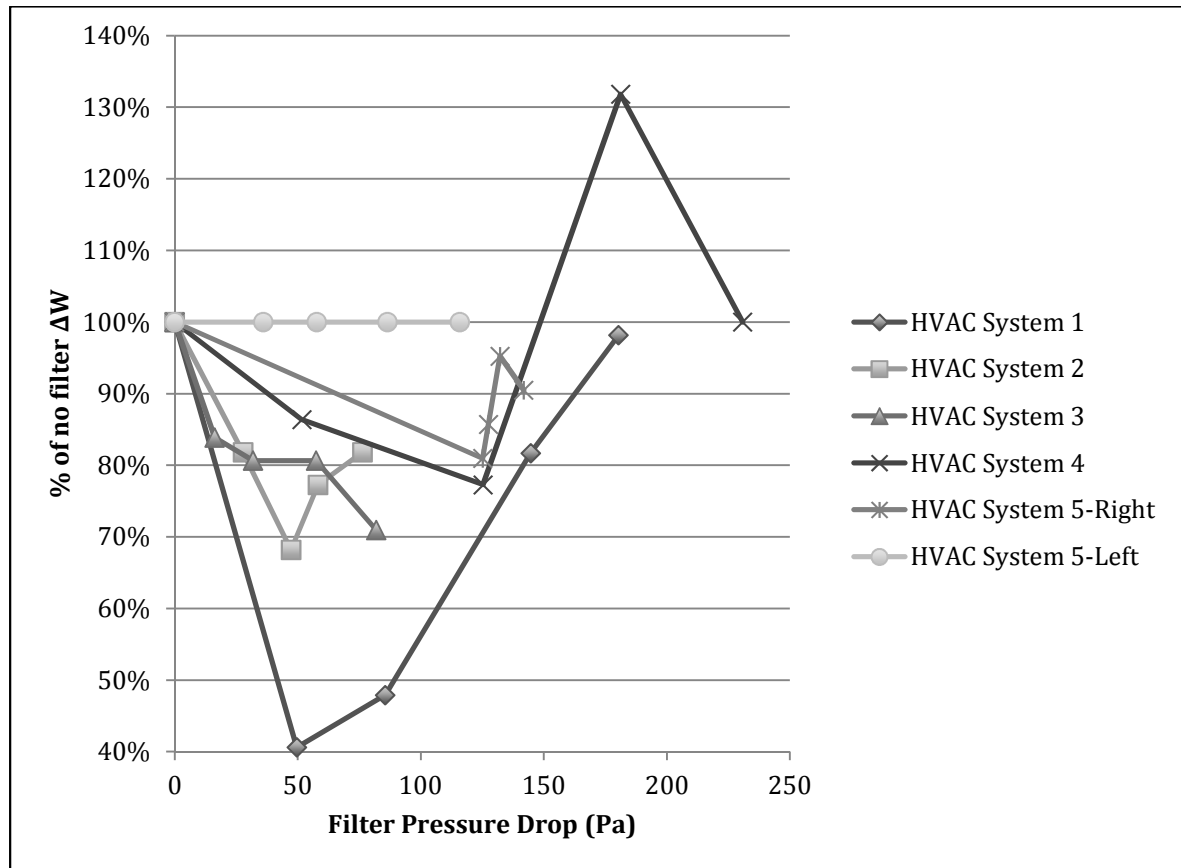


Figure 23 Relationship of filter pressure drop and  $\Delta W$  for each test systems.

Figure 24 shows the same  $\Delta W$  and filter pressure data measured at each site and induced loading condition, combined across all data points and fitted with a linear regression. Regression analysis shows a slope near zero and a coefficient of determination ( $R^2$ ) of only 0.01, suggesting that there was no observed correlation between filter pressure drop and  $\Delta W$ .

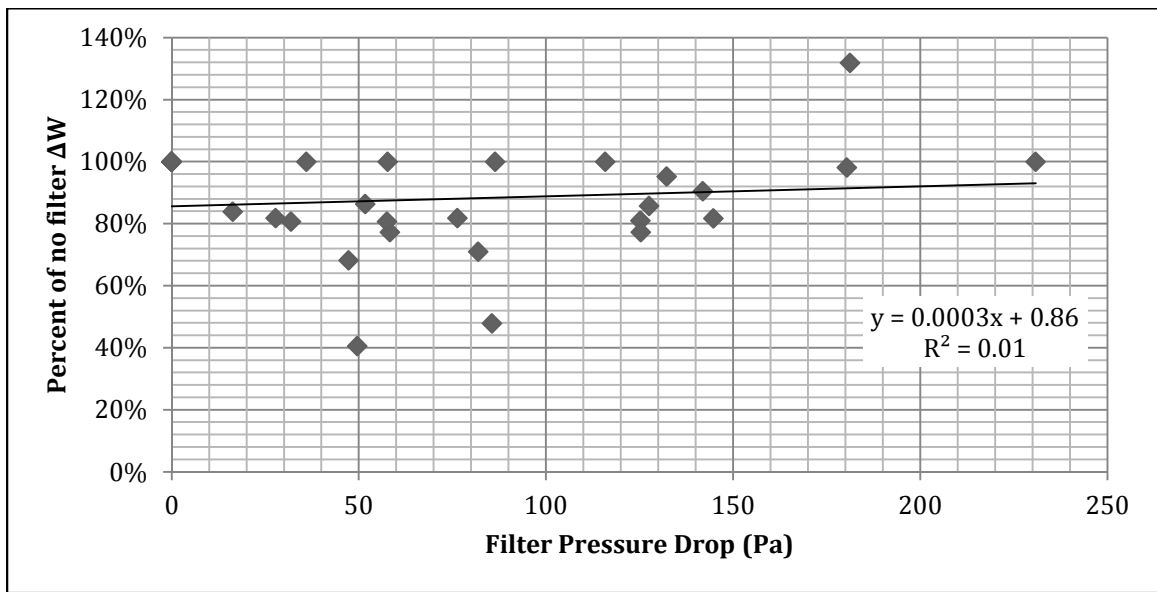


Figure 24 Relationship of filter pressure drop and  $\Delta W$  for all systems.

### Airflow and Temperature Differences Across the Coil

Because airflow rates and pressure drops were not necessarily directly correlated, this section explores the relationship of airflow rate (instead of pressure drop) and the dry bulb temperature difference across the evaporator coil ( $\Delta T$ ) in each system, as shown in Table 9 and Figure 25. The difference in temperature ( $\Delta T$ ) before passing the evaporator coil (pre-filter) and after passing the coil (in supply plenum) was measured. Values of ( $\Delta T$ ) at each flow and pressure drop condition were normalized to those measured with no filter installed and compared to the absolute value of the pressure drop across the filter. The change in  $\Delta T$  ranged from 152% of total system airflow (i.e. the difference in



temperature increased) to 97% (i.e., a 3% reduction in  $\Delta T$ ). The reduced airflow ranged from 100% of total system airflow (i.e. airflow remained unchanged) to 61%.

Table 9 Fractional airflow and changes in  $\Delta T$  across the evaporator coil

HVAC System Name	Percent of no filter flow (%)					Percent of no filter $\Delta T$ (%)				
	No Filter	True Flow	True Flow Taped 1	True Flow Taped 2	True Flow Taped 3	No Filter	True Flow	True Flow Taped 1	True Flow Taped 2	True Flow Taped 3
1	100%	93%	89%	77%	69%	100%	94%	100%	108%	123%
2	100%	98%	96%	94%	97%	100%	102%	107%	107%	110%
3	100%	100%	98%	95%	90%	100%	108%	110%	113%	113%
4	100%	88%	82%	73%	61%	100%	102%	111%	152%*	138%
5 (Right)	100%	97%	95%	91%	83%	100%	97%	98%	98%	97%
6 (5-Left)	100%	100%	99%	99%	99%	100%	107%	109%	111%	114%

\* Data point is statistically an outlier and removed from analysis.

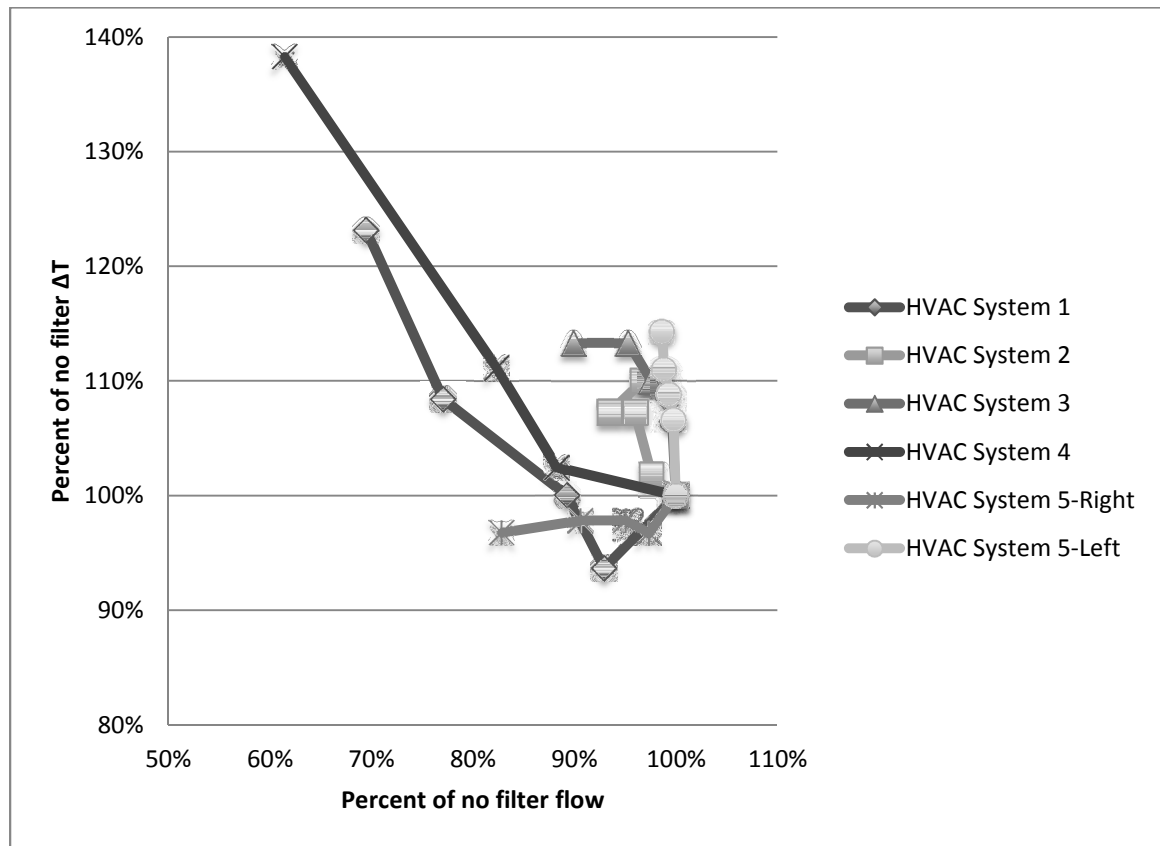


Figure 25 Relationship of airflow and  $\Delta T$  for each system.

Similarly, Figure 26 shows the same  $\Delta T$  and system airflow data measured at each site and induced loading condition, combined across all data points and fit with a linear regression. Regression analysis shows an intercept near 0.80, a slope of 1.81, and a coefficient of determination ( $R^2$ ) of 0.44, suggesting that with moderate certainty, each additional 10% decrease in system airflow resulted in a ~9.8% increase in system  $\Delta T$  in these systems.

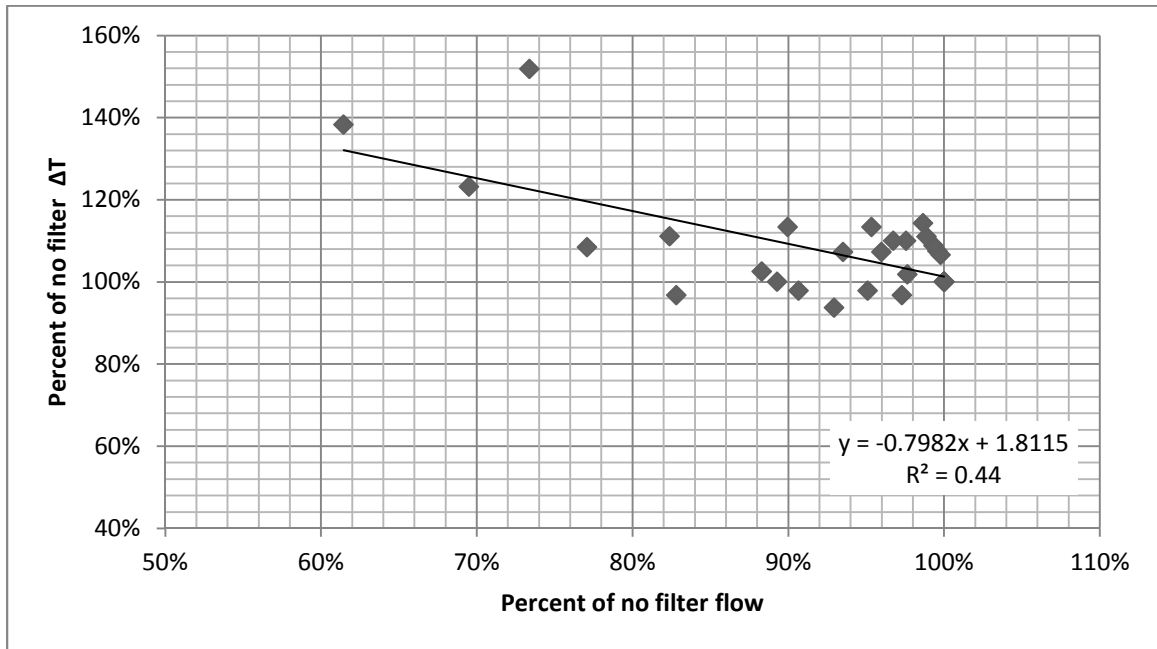


Figure 26 Relationship of airflow and  $\Delta T$  for all systems.

These data suggest what other laboratory and field studies have shown: as airflow rates are reduced in the presence of larger filter pressure drops, temperature difference across the coil increases slightly and supply air is delivered at a lower temperature (Nassif 2012, Yang et al 2004). This data also shows that there is a stronger relationship between  $\Delta T$  and airflow as opposed to  $\Delta T$  and induced filter pressure drop ( $R^2 = 0.44$  vs. 0.29). This is plausible because induced filter pressure drop affects airflow differently in each system, and  $\Delta T$  is directly impacted by airflow (and not necessarily pressure drop).

### Airflow and Absolute Humidity Differences Across the Coil

The relationship between system airflow and changes in the difference in absolute humidity across the coil ( $\Delta W$ ) was evaluated in each system, as shown in Table 10. Because  $\Delta W$  was calculated using the dry bulb temperature and relative humidity measurements in each location, data from True Flow Taped 2 in System 4 was again excluded as an outlier. The resulting changes in  $\Delta W$  ranged from a minimum of 41% (i.e. a 59% reduction in  $\Delta W$ ) to a maximum of 100% (i.e.  $\Delta W$  did not change). The reduced airflow ranged from 100% of total system airflow (i.e. airflow remained unchanged) to 61% (i.e. a 39% reduction in airflow). These data are shown in Figure 27 for each test system.

Table 10 System airflow and  $\Delta W$  across the evaporator coil

HVAC System Name	Percent of no filter $\Delta W$ (%)					Percent of no filter flow (%)				
	No Filter	True Flow	True Flow Taped 1	True Flow Taped 2	True Flow Taped 3	No Filter	True Flow	True Flow Taped 1	True Flow Taped 2	True Flow Taped 3
1	100%	41%	48%	82%	98%	100%	93%	89%	77%	69%
2	100%	82%	68%	77%	82%	100%	98%	96%	94%	97%
3	100%	84%	81%	81%	71%	100%	100%	98%	95%	90%
4	100%	86%	77%	132%	100%	100%	88%	82%	73%	61%
5 (Right)	100%	81%	86%	95%	90%	100%	97%	95%	91%	83%
6 (5-Left)	100%	100%	100%	100%	100%	100%	100%	99%	99%	99%

\*This data point is statistically an outlier and removed from analysis.

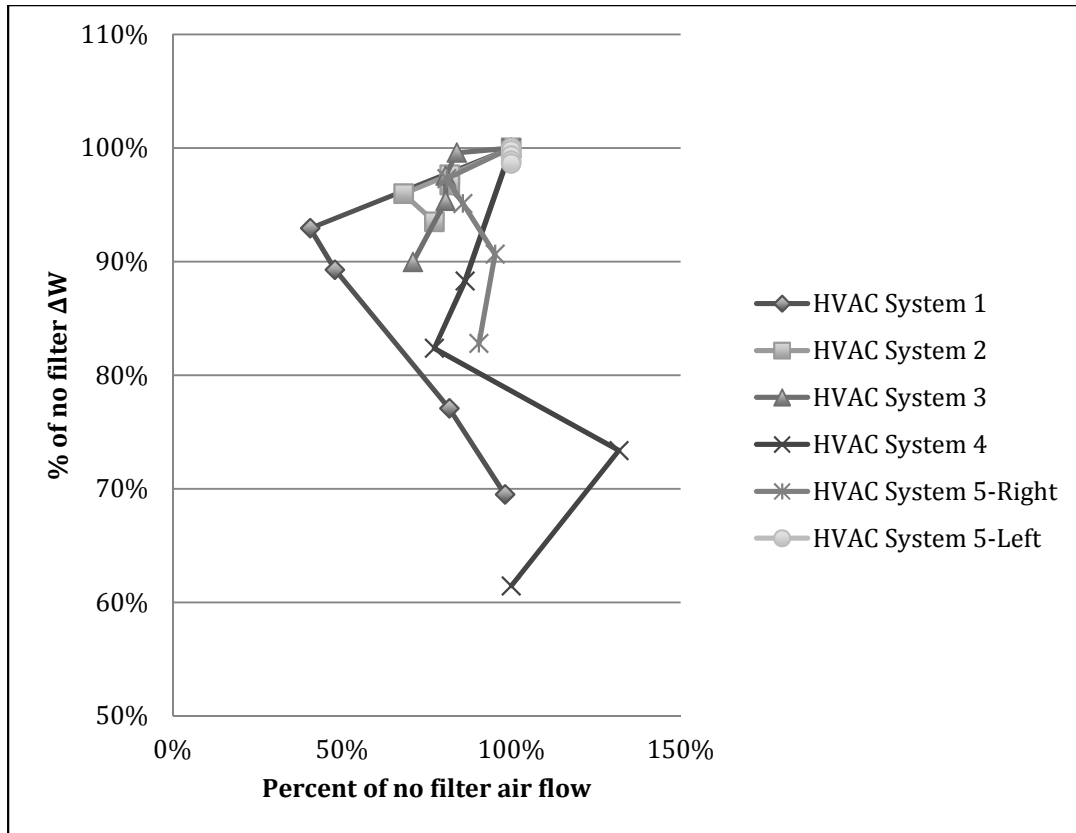


Figure 27 The relationship of airflow and absolute humidity for each system.

Similarly, Figure 28 shows the same  $\Delta W$  and system airflow data measured at each site and simulated loading condition, combined across all data points and fit with a linear regression. Regression analysis shows an intercept near 0.98, a slope of 0.07, and a coefficient of determination ( $R^2$ ) of 0.02, suggesting no correlation between system airflow and  $\Delta W$ .

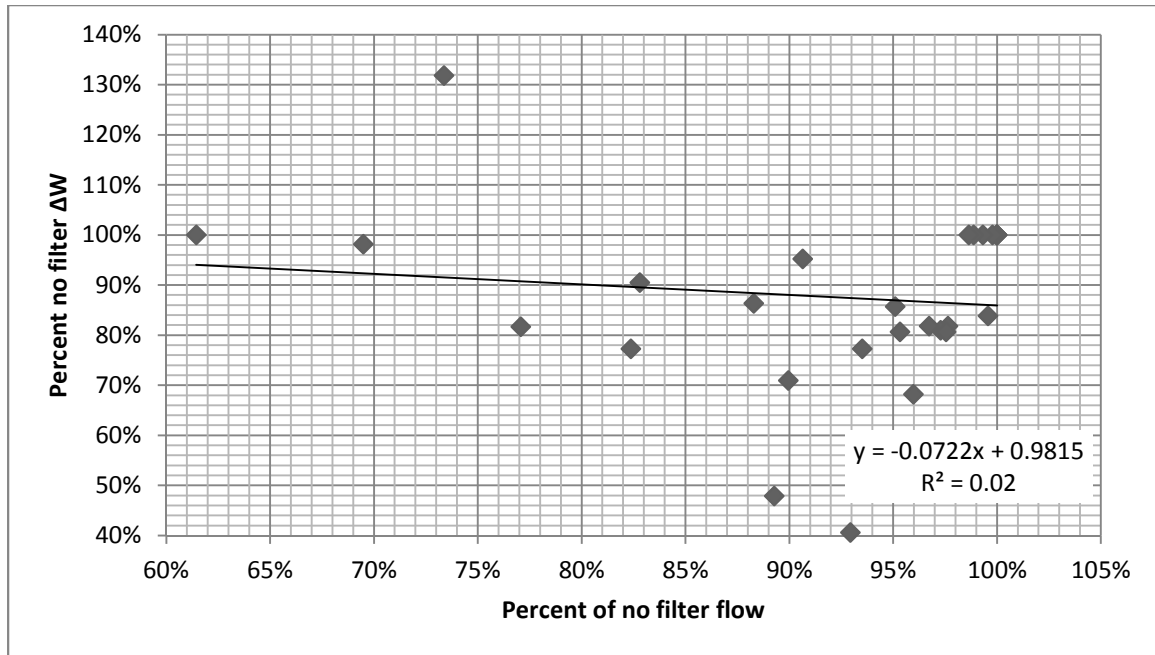


Figure 28 Relationship of airflow and absolute humidity for all systems.

### Airflow and System Capacity

The change in sensible, latent, and total capacities (as a percent of system capacity with no filter installed) was compared to the reduction in airflow (as a percent of total system flow without filter installed), as shown in Table 11. The reduced airflow ranged from 100% of total system airflow (i.e. airflow remained unchanged) to 61% (i.e. the airflow decreased by 39%). The change in sensible capacity ranged from 108% to 80%.

Table 11 Relationship of airflow and sensible capacity for all systems.

HVAC System Name	Percent of no filter flow (%)					Percent no Filter Sensible Capacity (kBtu/hr)				
	No Filter	True Flow	True Flow Taped 1	True Flow Taped 2	True Flow Taped 3	No Filter	True Flow	True Flow Taped 1	True Flow Taped 2	True Flow Taped 3
1	100%	93%	89%	77%	69%	100%	87%	89%	84%	86%
2	100%	98%	96%	94%	97%	100%	99%	103%	100%	106%
3	100%	100%	98%	95%	90%	100%	107%	107%	108%	102%
4	100%	88%	82%	73%	61%	100%	90%	92%	111%	85%
5-Right	100%	97%	95%	91%	83%	100%	94%	93%	89%	80%
5-Left	100%	100%	99%	99%	99%	100%	106%	108%	110%	113%

\* Data point is statistically an outlier and removed from analysis.

Similarly, Figure 29 shows the same sensible capacity and system airflow data measured at each site and simulated loading condition, combined across all data points and fit with a linear regression. Regression analysis shows an intercept near 0.36, a slope of 0.67, and a coefficient of determination ( $R^2$ ) of 0.53, suggesting that with moderate certainty, each 10% reduction in airflow resulted in a ~7% decrease in sensible capacity in these systems. If one was concerned with keeping sensible capacity at least 80% of the no filter sensible capacity, these data suggest that airflow rates should not be able to decrease more than approximately 30%.

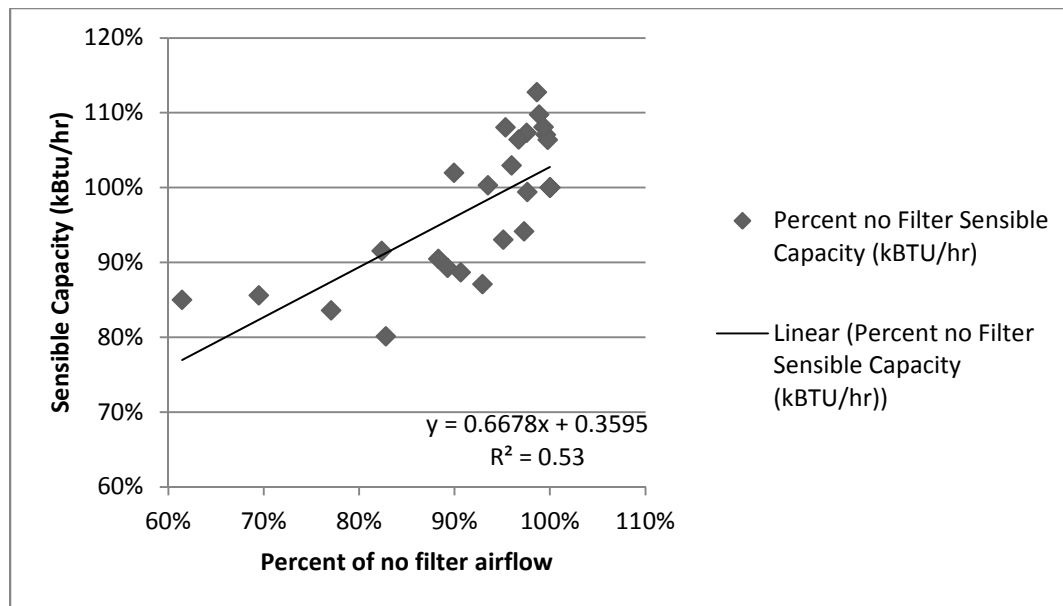


Figure 29 Relationship of airflow and sensible capacity for all systems.

The change in latent capacity ranged from 100% to 38% (Table 12). Figure 30 shows the same latent capacity and system airflow data measured at each site and simulated loading condition, combined across all data points and fit with a linear regression. Regression analysis shows an intercept near 0.04, a slope of 0.84, and a coefficient of determination ( $R^2$ ) of 0.23, suggesting that with relatively low certainty, a 10% decrease in airflow resulted in a ~10.4% decrease in system latent capacity in these systems.

Table 12 Relationship of airflow and latent capacity for all systems.

HVAC System Name	Percent of no filter flow (%)					Percent no Filter Latent Capacity (kBTU/hr)				
	No Filter	True Flow	True Flow Taped 1	True Flow Taped 2	True Flow Taped 3	No Filter	True Flow	True Flow Taped 1	True Flow Taped 2	True Flow Taped 3
1	100%	93%	89%	77%	69%	100%	38%	43%	63%	68%
2	100%	98%	96%	94%	97%	100%	80%	65%	72%	79%
3	100%	100%	98%	95%	90%	100%	84%	79%	77%	64%
4	100%	88%	82%	73%	61%	100%	76%	64%	97%	61%
5-Right	100%	97%	95%	91%	83%	100%	79%	82%	86%	75%
5-Left	100%	100%	99%	99%	99%	100%	100%	99%	99%	99%

\* Data point is statistically an outlier and removed from analysis.

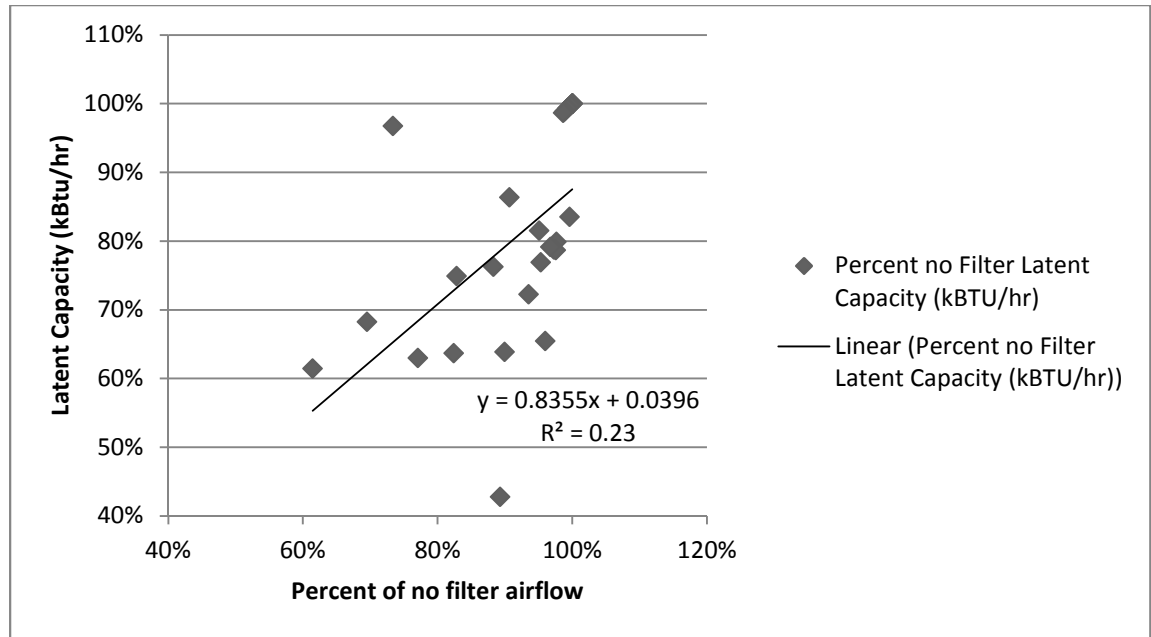


Figure 30 Relationship of airflow and latent capacity for all systems.

Finally, the change in total capacity ranged from 108% to 69% (Table 13). Figure 31 shows the same latent capacity and system airflow data measured at each site and simulated loading condition, combined across all data points and fit with a linear regression. Regression analysis shows an intercept near 0.33, a slope of 0.64, and a coefficient of determination ( $R^2$ ) of 0.36, suggesting that with moderate certainty, each additional 10% reduction in airflow resulted in a ~6.7% decrease in total cooling capacity in these systems.

Table 13 Relationship of airflow and total capacity for all systems.

HVAC System Name	Percent of no filter flow (%)					Percent no Filter Total Capacity (kBtu/hr)				
	No Filter	True Flow	True Flow Taped 1	True Flow Taped 2	True Flow Taped 3	No Filter	True Flow	True Flow Taped 1	True Flow Taped 2	True Flow Taped 3
1	100%	93%	89%	77%	69%	100%	69%	72%	76%	79%
2	100%	98%	96%	94%	97%	100%	93%	91%	92%	98%
3	100%	100%	98%	95%	90%	100%	98%	97%	97%	88%
4	100%	88%	82%	73%	61%	100%	85%	81%	106%	76%
5-Right	100%	97%	95%	91%	83%	100%	89%	89%	88%	78%
5-Left	100%	100%	99%	99%	99%	100%	104%	105%	106%	108%

\* Data point is statistically an outlier and removed from analysis.

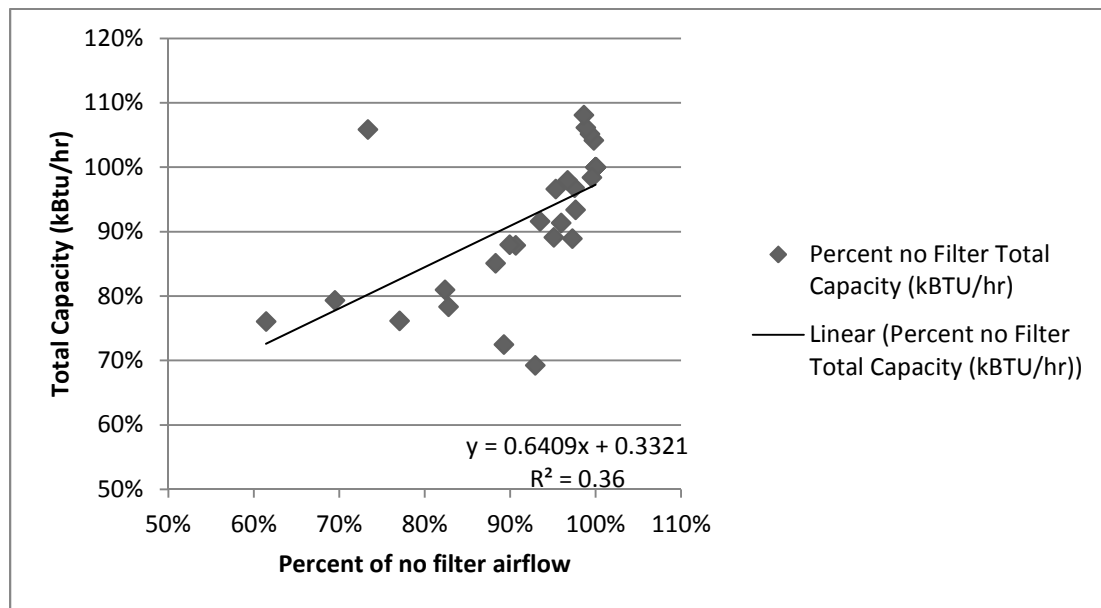


Figure 31 Relationship of airflow and total capacity for all systems.



These data suggest what other laboratory and field studies have shown: as airflow rates are reduced in the presence of larger filter pressure drops, total cooling capacity is reduced. Rodriguez et al. (1996) showed that a 10% reduction in airflow caused capacity to decrease by approximately 7% in a laboratory setting. Stephens et al (2010) found that decreasing airflow rates by approximately 7% results in only a 3-4% reduction in total capacity in field measurements in a controlled test house setting. These are some of the first data to systematically report changes in capacity in response to simulated filter loading conditions in real residences.

In other words, as airflow decreased so did sensible, latent, and total capacity, although these relationships were not linear. Because reductions in cooling capacity can be linked to increased system runtimes, this research can be used to inform decisions about maximum filter loading values that should inform filter replacement schedules. Once a maximum acceptable reduction in sensible capacity is established, this data can be used to identify the airflow and filter pressure drop thresholds, which can impact future decisions about filter replacement timing.

Data herein can be used to inform filter replacement strategies in U.S. homes. Once a maximum acceptable reduction in sensible capacity is established, this data can be used to identify the airflow and filter pressure drop thresholds, which can impact future decisions about filter replacement timing. Taking values relative to no filter conditions (for which 100% flow is impossible in most systems because even the lowest efficiency filter will induce more pressure drop than no filter conditions), one could define, say, a 20% reduction in sensible capacity relative to no filter conditions as the maximum allowable value. This sensible capacity reduction is an admittedly arbitrary value that should be verified in energy simulations and field tests. According to the data in Figure 29, sensible capacity is reduced to 80% of no filter sensible capacity when airflow is reduced by approximately 30% to only 70% of the no filter airflow. According to Figure 20, a 30% reduction in airflow would occur at a filter pressure drop of approximately 225

Pa. Similarly, if only a 10% reduction in sensible capacity was set as the criteria, a maximum of approximately 15% reduction in airflow (relative to no filter) would be allowed, which would be reached a filter pressure drop of approximately 125 Pa.

Although these criteria should be further refined with simulations and larger field studies, the methods and results herein suggest that enough information can be gathered to establish maximum filter pressure drops allowed in residential HVAC systems, and particularly in those that rely on blowers without sophisticated flow controls.

## **CHAPTER 5**

### **CONCLUSION**

This study sought to: (i) develop and apply a methodology for simulating filter loading in-situ; (ii) measure the impact of simulated filter loading on air conditioner (AC) performance in-situ; and (iii) provide a greater understanding of when a filter is “dirty” and in should be replaced. Five central AC systems in the Atlanta metro-region were evaluated using TrueFlow from The Energy Conservatory. Filter loading was simulated by installing the TrueFlow® airflow metering device and partially taping off the face at three different increments. This resulted in measurements at five discrete static pressure conditions: no filter, TrueFlow, TrueFlow Taped #1, TrueFlow Taped #2, and TrueFlow Taped #3. The results strongly suggest that this methodology is an accurate means of simulating filter loading in-situ and provides important HVAC performance data. Results from each major section are summarized below.

#### **Filter Pressure Drop & System Airflow**

The relationship between induced filter pressure drop and system airflow rates was first evaluated in each system. The absolute value of the pressure drop across the filter was compared to the reduction in airflow (as a percentage of total system flow without filter installed) for each induced pressure drop condition. Overall, as filter pressure drop increased, airflow rates generally decreased, particularly for the known PSC blowers. The two systems that were apparently ECM blowers (or at least variable speed blowers) responded to increased filter pressure drop by nearly maintaining airflow rates until reaching a maximum pressure and rapidly decreasing in flow, which is consistent with other ECM data.

### **Filter Pressure Drop & Temperature Difference Across the Coil**

The relationship between induced filter pressure drop and the dry bulb temperature difference across the evaporator coil ( $\Delta T$ ) was evaluated in each system. The difference in temperature ( $\Delta T$ ) before passing the evaporator coil (pre-filter) and after passing the coil (in supply plenum) was measured. With moderate certainty, it was concluded that as induced filter pressure drop increased, the  $\Delta T$  also increased in these systems. These data suggest what other laboratory and field studies have shown: as airflow rates are reduced in the presence of larger filter pressure drops, sensible capacity will not decrease linearly with flow because the temperature difference across the coil increases slightly and supply air is delivered at a lower temperature. This section also further indicated the validity of this methodology for simulating filter loading in-situ.

### **Filter Pressure Drop & Absolute Humidity**

The relationship between induced filter pressure drop and changes in the difference in absolute humidity across the coil ( $\Delta W$ ) was evaluated in each system. The change in  $\Delta W$  across the coil (as a percentage of  $\Delta W$  without filter installed) was compared to the absolute value of the pressure drop across the filter for each induced pressure drop condition. There was no observed correlation between filter pressure drop and  $\Delta W$ .

### **Airflow and Temperature**

The relationship of airflow and the dry bulb temperature difference across the evaporator coil ( $\Delta T$ ) was evaluated in each system. The difference in temperature ( $\Delta T$ ) before passing the evaporator coil (pre-filter) and after passing the coil (in supply plenum) was measured. These data suggest what other laboratory and field studies have shown: as airflow rates are reduced in the presence of larger filter pressure drops, temperature difference across the coil increases slightly and supply air is delivered at a

lower temperature. This data also indicates that there is a stronger relationship between  $\Delta T$  and airflow rates compared to induced filter pressure drop because induced filter pressure drop did not affect airflow similarly in each system and it is airflow rates that directly impact  $\Delta T$ .

### **Airflow and Absolute Humidity**

The relationship between system airflow and changes in the difference in absolute humidity across the coil ( $\Delta W$ ) was evaluated in each system. There was no observed correlation between system airflow and  $\Delta W$ .

### **Airflow and System Capacity**

The change in sensible, latent, and total capacities (as a percent of system capacity with no filter installed) was compared to the reduction in airflow (as a percent of total system flow without filter installed). Overall as airflow decreased in response to larger filter pressure drops, so did sensible, latent, and total capacity, although impacts were not necessarily linear.

### **Analysis Summary**

Based on a relatively strong linear regression of system airflow versus induced filter pressure drop, airflow rates were reduced 10% from no filter airflow at around 90 Pa and reduced 20% from no filter airflow at around 150 Pa. This data can inform decisions about filter replacement and be used to educate builders, contractors, and homeowners about the importance of routine HVAC maintenance. Once a maximum acceptable reduction in sensible capacity is established, this data can be used to identify the airflow and filter pressure drop thresholds. For example, a 10% reduction in sensible capacity would result in approximately a 10% increase in AC run time, all is being equal. If a 10% reduction in sensible capacity is selected as the threshold for filter replacement,

then the data indicates filters should be replaced at around 80-85% of no filter airflow, which is around a filter pressure drop of 150 Pa.

### **Recommendations**

This pilot study provided valuable proof of concept for an approach to simulating filter loading in-situ. Taping the face of the TrueFlow was identified to work consistently well to simulate filter loading. In the future, the study should be expanded to a greater number of central air conditioners and continuous measurements should be recorded using data loggers. One challenge was establishing when the AC reached steady state. Greater certainty may be possible by recording continuous measurements and waiting longer between each simulated filter condition. Measuring the air handler and condenser power draw would also provide potentially valuable data. Additionally, the in-situ AC performance data can be used to evaluate and improve current computer models of HVAC performance.

## APPENDIX A

### TEST SYSTEM 1

	No Filter	True Flow	True Flow Taped 1	True Flow Taped 2	True Flow Taped 3
<b>Supply Measurements</b>					
Relative humidity, $\Phi$ (fractional)	0.89	0.92	0.93	0.92	0.93
Dry-bulb temperature, $t$ ( $^{\circ}\text{C}$ )	12.80	13.20	12.50	11.50	10.00
Humidity ratio, $W$ (kgw/kgda)	0.01	0.01	0.01	0.01	0.01
<b>Return Measurements</b>					
Relative humidity, $\Phi$ (fractional)	0.63	0.62	0.61	0.60	0.58
Dry-bulb temperature, $t$ ( $^{\circ}\text{C}$ )	22.30	22.10	22.00	21.80	21.70
pressure wrt outside	67.50	58.30	53.80	40.10	32.60
Humidity ratio, $W$ (kgw/kgda)	0.01	0.01	0.01	0.01	0.01
<b>Filter Measurement</b>					
Pressure (Coil Side)	67.50	107.90	139.40	184.80	213.00
Pfilt (pa)	0.00	49.60	85.60	144.70	180.40
True Flow Pressure (Pa)	-	62	-	-	-
True Flow Air Flow (CFM)	-	906	-	-	-
Adjusted airflow (CFM)	975	906	870	751	677
Percent of no filter flow	100%	93%	89%	77%	69%
deltaW	0.002	0.001	0.001	0.002	0.002
Percent of no filter deltaW	100.00%	40.60%	47.91%	81.70%	98.16%
deltaT	9.50	8.90	9.50	10.30	11.70
Percent of no filter deltaT	100.00%	93.68%	100.00%	108.42%	123.16%
<b>System Capacity</b>					
Qfan (m3/s)	0.46	0.43	0.41	0.35	0.32
Air density ( $p$ , kg/m3)	1.2	1.2	1.2	1.2	1.2
Specific heat of air ( $C$ , kJ/(kgK)	1.005	1.005	1.005	1.005	1.005
deltaT (K)	9.50	8.90	9.50	10.30	11.70
deltaW (kg/kg)	0.002	0.001	0.001	0.002	0.002
Hfg (kJ/kg)	2257	2257	2257	2257	2257
Sensible Capacity (kW)	5.27	4.59	4.71	4.40	4.51
Latent Capacity (kW)	2.98	1.13	1.28	1.88	2.04
Total Capacity (kW)	8.25	5.72	5.98	6.28	6.55
Sensible Capacity (kBTU/hr)	17.99	15.66	16.06	15.03	15.39
Latent Capacity (kBTU/hr)	10.18	3.84	4.35	6.41	6.94
Total Capacity (kBTU/hr)	28.16	19.50	20.41	21.44	22.34
Sensible Capacity (tons)	1.50	1.30	1.34	1.25	1.28
Latent Capacity (tons)	0.85	0.32	0.36	0.53	0.58
Total Capacity (tons)	2.35	1.62	1.70	1.79	1.86
Percent no filter Sensible Capacity	100.00%	87.07%	89.28%	83.57%	85.59%
Percent no filter Latent Capacity	100.00%	37.73%	42.77%	62.97%	68.22%
Percent no filter Total Capacity	100.00%	69.24%	72.47%	76.12%	79.31%

## TEST SYSTEM 2

	No Filter	True Flow	True Flow Taped 1	True Flow Taped 2	True Flow Taped 3
<b>Supply Measurements</b>					
Relative humidity, $\Phi$ (fractional)	0.85	0.87	0.86	0.87	0.87
Dry-bulb temperature, $t$ ( $^{\circ}\text{C}$ )	9.40	8.40	7.30	6.90	6.30
Humidity ratio, $W$ (kgw/kgda)	0.01	0.01	0.01	0.01	0.01
pressure wrt house	79.80	78.10	75.00	72.40	69.10
<b>Return Measurements</b>					
Relative humidity, $\Phi$ (fractional)	0.56	0.55	0.51	0.52	0.53
Dry-bulb temperature, $t$ ( $^{\circ}\text{C}$ )	20.40	19.60	19.10	18.70	18.40
pressure wrt house	62.10	59.20	57.20	54.30	53.30
Humidity ratio, $W$ (kgw/kgda)	0.0084	0.0078	0.0070	0.0070	0.0069
<b>Filter Measurement</b>					
Pressure (Coil Side)		87	104.5	112.6	129.6
Pfilt (pa)	0	27.8	47.3	58.3	76.3
True Flow Pressure (Pa)	-	34	-	-	-
True Flow Air Flow (CFM)	-	674	-	-	-
Adjusted airflow (CFM)	690	674	663	646	668
Percent of no filter flow	100.00%	97.64%	95.97%	93.51%	96.73%
deltaW	0.002	0.002	0.002	0.002	0.002
Percent of no filter deltaW	100.00%	81.82%	68.18%	77.27%	81.82%
deltaT	11.00	11.20	11.80	11.80	12.10
Percent of no filter deltaT	100.00%	101.82%	107.27%	107.27%	110.00%
<b>System Capacity</b>					
Qfan (m3/s)	0.33	0.32	0.31	0.30	0.32
Air density ( $\rho$ , kg/m3)	1.2	1.2	1.2	1.2	1.2
Specific heat of air ( $C$ , kJ/(kgK))	1.005	1.005	1.005	1.005	1.005
deltaT (K)	11.00	11.20	11.80	11.80	12.10
deltaW (kg/kg)	0.002	0.002	0.002	0.002	0.002
Hfg (kJ/kg)	2257	2257	2257	2257	2257
Sensible Capacity (kW)	4.32	4.30	4.45	4.34	4.60
Latent Capacity (kW)	1.94	1.55	1.27	1.40	1.54
Total Capacity (kW)	6.26	5.85	5.72	5.74	6.14
Sensible Capacity (kBTU/hr)	14.75	14.66	15.18	14.79	15.69
Latent Capacity (kBTU/hr)	6.62	5.29	4.33	4.79	5.24
Total Capacity (kBTU/hr)	21.37	19.95	19.52	19.58	20.93
Sensible Capacity (tons)	1.23	1.22	1.27	1.23	1.31
Latent Capacity (tons)	0.55	0.44	0.36	0.40	0.44
Total Capacity (tons)	1.78	1.66	1.63	1.63	1.74
Percent no filter Sensible Capacity	100.00%	99.41%	102.95%	100.31%	106.41%
Percent no filter Latent Capacity	100.00%	79.88%	65.44%	72.26%	79.15%
Percent no filter Total Capacity	100.00%	93.36%	91.33%	91.62%	97.96%



### TEST SYSTEM 3

	No Filter	True Flow	True Flow Taped 1	True Flow Taped 2	True Flow Taped 3
<b>Supply Measurements</b>					
Relative humidity, $\Phi$ (fractional)	0.833	0.837	0.837	0.837	0.834
Dry-bulb temperature, $t$ (°C)	11.30	9.60	9.00	8.30	8.10
Humidity ratio, $W$ (kgw/kgda)	0.007	0.006	0.006	0.006	0.006
pressure wrt attic	133.20	130.30	125.80	118.90	107.60
<b>Return Measurements</b>					
Relative humidity, $\Phi$ (fractional)	0.561	0.521	0.513	0.504	0.501
Dry-bulb temperature, $t$ (°C)	23.30	22.50	22.20	21.90	21.70
pressure wrt attic	35.10	34.80	33.40	31.90	28.40
Humidity ratio, $W$ (kgw/kgda)	0.0100	0.0088	0.0085	0.0082	0.0080
<b>Filter Measurement</b>					
Pressure (Coil Side)		51.1	65.3	89.4	110.3
Pfilt (pa)	0	16.3	31.9	57.5	81.9
True Flow Pressure (Pa)	-	16.7	-	-	-
True Flow Air Flow (CFM)	-	474	-	-	-
Adjusted airflow (CFM)	476	474	464	454	428
Percent of no filter flow	100.00%	99.57%	97.55%	95.33%	89.95%
deltaW	0.003	0.003	0.003	0.003	0.002
Percent of no filter deltaW	100.00%	83.87%	80.65%	80.65%	70.97%
deltaT	12.00	12.90	13.20	13.60	13.60
Percent of no filter deltaT	100.00%	107.50 %	110.00%	113.33%	113.33%
<b>System Capacity</b>					
Qfan (m3/s)	0.225	0.224	0.219	0.214	0.202
Air density ( $p$ , kg/m3)	1.2	1.2	1.2	1.2	1.2
Specific heat of air ( $C$ , kJ/(kgK)	1.005	1.005	1.005	1.005	1.005
deltaT (K)	12.00	12.90	13.20	13.60	13.60
deltaW (kg/kg)	0.003	0.003	0.003	0.003	0.002
Hfg (kJ/kg)	2257	2257	2257	2257	2257
Sensible Capacity (kW)	3.25	3.48	3.49	3.51	3.31
Latent Capacity (kW)	1.89	1.58	1.48	1.45	1.20
Total Capacity (kW)	5.14	5.06	4.97	4.96	4.52
Sensible Capacity (kBTU/hr)	11.09	11.87	11.90	11.99	11.31
Latent Capacity (kBTU/hr)	6.44	5.37	5.06	4.95	4.11
Total Capacity (kBTU/hr)	17.53	17.25	16.97	16.93	15.42
Sensible Capacity (tons)	0.92	0.99	0.99	1.00	0.94
Latent Capacity (tons)	0.54	0.45	0.42	0.41	0.34
Total Capacity (tons)	1.46	1.44	1.41	1.41	1.28
Percent no filter Sensible Capacity	100.00%	107.04 %	107.30%	108.04%	101.94%
Percent no filter Latent Capacity	100.00%	83.51%	78.67%	76.88%	63.84%
Percent no filter Total Capacity	100.00%	98.40%	96.79%	96.60%	87.95%

## TEST SYSTEM 4

	No Filter	True Flow	True Flow Taped 1	True Flow Taped 2	True Flow Taped 3
<b>Supply Measurements</b>					
Relative humidity, $\Phi$ (fractional)	0.805	0.817	0.859	0.874	0.882
Dry-bulb temperature, $t$ (°C)	15.20	14.30	13.30	9.40	10.00
Humidity ratio, $W$ (kgw/kgda)	0.009	0.008	0.008	0.006	0.007
pressure wrt outside	26.80	23.20	20.80	15.20	11.80
<b>Return Measurements</b>					
Relative humidity, $\Phi$ (fractional)	0.612	0.597	0.589	0.575	0.565
Dry-bulb temperature, $t$ (°C)	23.30	22.60	22.30	21.70	21.20
pressure wrt outside	53.50	41.70	36.30	28.80	20.20
Humidity ratio, $W$ (kgw/kgda)	0.011	0.010	0.010	0.009	0.009
<b>Filter Measurement</b>					
Pressure (Coil Side)	-	93.4	161.6	210	251
Pfilt (pa)	0	51.7	125.3	181.2	230.8
True Flow Pressure (Pa)	-	69	-	-	-
True Flow Air Flow (CFM)	-	1279	-	-	-
Adjusted airflow (CFM)	1449	1279	1193	1063	890
Percent of no filter flow	100.00%	88.29%	82.37%	73.37%	61.45%
deltaW	0.002	0.002	0.002	0.003	0.002
Percent of no filter deltaW	100.00%	86.36%	77.27%	131.82%	100.00%
deltaT	8.10	8.30	9.00	12.30	11.20
Percent of no filter deltaT	100.00%	102.47%	111.11%	151.85%	138.27%
<b>System Capacity</b>					
Qfan (m3/s)	0.68	0.60	0.56	0.50	0.42
Air density ( $\rho$ , kg/m3)	1.2	1.2	1.2	1.2	1.2
Specific heat of air ( $C$ , kJ/(kgK))	1.005	1.005	1.005	1.005	1.005
deltaT (K)	8.10	8.30	9.00	12.30	11.20
deltaW (kg/kg)	0.002	0.002	0.002	0.003	0.002
Hfg (kJ/kg)	2257	2257	2257	2257	2257
Sensible Capacity (kW)	6.68	6.04	6.11	7.44	5.67
Latent Capacity (kW)	4.07	3.11	2.59	3.94	2.50
Total Capacity (kW)	10.75	9.15	8.71	11.38	8.18
Sensible Capacity (kBTU/hr)	22.79	20.62	20.86	25.39	19.36
Latent Capacity (kBTU/hr)	13.90	10.60	8.85	13.44	8.54
Total Capacity (kBTU/hr)	36.69	31.21	29.70	38.83	27.90
Sensible Capacity (tons)	1.90	1.72	1.74	2.12	1.61
Latent Capacity (tons)	1.16	0.88	0.74	1.12	0.71
Total Capacity (tons)	3.06	2.60	2.48	3.24	2.33
Percent no filter Sensible Capacity	100.00%	90.47%	91.52%	111.41%	84.96%
Percent no filter Latent Capacity	100.00%	76.25%	63.65%	96.72%	61.45%
Percent no filter Total Capacity	100.00%	85.08%	80.96%	105.85%	76.05%

## TEST SYSTEM 5

<b>Supply Measurements</b>	<b>No Filter</b>	<b>True Flow</b>	<b>True Flow Taped 1</b>	<b>True Flow Taped 2</b>	<b>True Flow Taped 3</b>
Relative humidity, $\Phi$ (fractional)	0.876	0.883	0.88	0.885	0.887
Dry-bulb temperature, $t$ (°C)	11.60	11.60	11.40	11.40	11.30
Humidity ratio, $W$ (kgw/kgda)	0.0074	0.0075	0.0074	0.0074	0.0074
pressure wrt outside	63.5	62.8	62.5	62	59.9
<b>Return Measurements</b>					
Relative humidity, $\Phi$ (fractional)	0.621	0.613	0.617	0.632	0.628
Dry-bulb temperature, $t$ (°C)	20.8	20.5	20.4	20.4	20.2
pressure wrt outside	123.4	116.8	111.6	101.4	84.6
Humidity ratio, $W$ (kgw/kgda)	0.0095	0.0092	0.0092	0.0094	0.0093
<b>Filter Measurement</b>					
Pressure (Coil Side)	0	125.2	127.5	132.2	141.9
Pfilt (pa)	0	8.4	15.9	30.8	57.3
True Flow Pressure (Pa)	-	16.2	-	-	-
True Flow Air Flow (CFM)	-	616	-	-	-
Adjusted airflow (CFM)	633	616	602	574	524
Percent of no filter flow	100.00%	97.29%	95.10%	90.65%	82.80%
deltaW	0.002	0.002	0.002	0.002	0.002
Percent of no filter deltaW	100.00%	80.95%	85.71%	95.24%	90.48%
deltaT	9.20	8.90	9.00	9.00	8.90
Percent of no filter deltaT	100.00%	96.74%	97.83%	97.83%	96.74%
<b>System Capacity</b>					
Qfan (m3/s)	0.30	0.29	0.28	0.27	0.25
Air density ( $\rho$ , kg/m3)	1.2	1.2	1.2	1.2	1.2
Specific heat of air ( $C$ , kJ/(kgK))	1.005	1.005	1.005	1.005	1.005
deltaT (K)	9.20	8.90	9.00	9.00	8.90
deltaW (kg/kg)	0.002	0.002	0.002	0.002	0.002
Hfg (kJ/kg)	2257	2257	2257	2257	2257
Sensible Capacity (kW)	3.32	3.12	3.08	2.94	2.66
Latent Capacity (kW)	1.70	1.34	1.39	1.47	1.27
Total Capacity (kW)	5.02	4.46	4.47	4.41	3.93
Sensible Capacity (kBTU/hr)	11.3	10.6	10.5	10.0	9.1
Latent Capacity (kBTU/hr)	5.80	4.57	4.73	5.01	4.34
Total Capacity (kBTU/hr)	17.1	15.2	15.3	15.0	13.4
Sensible Capacity (tons)	0.94	0.89	0.88	0.84	0.76
Latent Capacity (tons)	0.48	0.38	0.39	0.42	0.36
Total Capacity (tons)	1.43	1.27	1.27	1.25	1.12
Percent no filter Sensible Capacity	100.00%	94.12%	93.03%	88.68%	80.10%
Percent no filter Latent Capacity	100.00%	78.76%	81.51%	86.33%	74.91%
Percent no filter Total Capacity	100.00%	88.91%	89.13%	87.88%	78.34%

## TEST SYSTEM 6

	No Filter	True Flow	True Flow Taped 1	True Flow Taped 2	True Flow Taped 3
<b>Supply Measurements</b>					
Relative humidity, $\Phi$ (fractional)	0.852	0.866	0.873	0.876	0.878
Dry-bulb temperature, $t$ (°C)	13.1	12.4	12.0	11.6	11.2
Humidity ratio, $W$ (kgw/kgda)	0.0080	0.0078	0.0076	0.0074	0.0073
pressure wrt outside	65.6	64.6	63.5	59.5	55.3
<b>Return Measurements</b>					
Relative humidity, $\Phi$ (fractional)	0.598	0.592	0.583	0.579	0.576
Dry-bulb temperature, $t$ (°C)	22.2	22.1	21.9	21.7	21.6
pressure wrt outside	95.3	82.6	75.9	68.8	60.6
Humidity ratio, $W$ (kgw/kgda)	0.010	0.010	0.010	0.009	0.009
<b>Filter Measurement</b>					
Pressure (Coil Side)	-	118.6	133.6	155.2	176.4
Pfilt (pa)	0	36	57.7	86.4	115.8
True Flow Pressure (Pa)	-	46	-	-	-
True Flow Air Flow (CFM)	-	1044	-	-	-
Adjusted airflow (CFM)	1046	1044	1039	1035	1032
Percent of no filter flow	100.00%	99.77%	99.32%	98.87%	98.64%
deltaW	0.002	0.002	0.002	0.002	0.002
Percent of no filter deltaW	100%	100.0%	100.0%	100.0%	100.0%
deltaT	9.100	9.700	9.900	10.100	10.400
Percent of no filter deltaT	100.00%	106.59%	108.79%	110.99%	114.29%
<b>System Capacity</b>					
Qfan (m3/s)	0.49	0.49	0.49	0.49	0.49
Air density ( $\rho$ , kg/m3)	1.2	1.2	1.2	1.2	1.2
Specific heat of air ( $C$ , kJ/(kgK))	1.005	1.005	1.005	1.005	1.005
deltaT (K)	9.10	9.70	9.90	10.10	10.40
deltaW (kg/kg)	0.0020	0.002	0.002	0.002	0.002
Hfg (kJ/kg)	2257	2257	2257	2257	2257
Sensible Capacity (kW)	5.42	5.76	5.86	5.95	6.11
Latent Capacity (kW)	2.67	2.67	2.66	2.64	2.64
Total Capacity (kW)	8.09	8.43	8.51	8.59	8.75
Sensible Capacity (kBtu/hr)	18.49	19.67	19.98	20.29	20.85
Latent Capacity (kBtu/hr)	9.13	9.11	9.07	9.02	9.00
Total Capacity (kBtu/hr)	27.62	28.77	29.05	29.31	29.85
Sensible Capacity (tons)	1.54	1.64	1.67	1.69	1.74
Latent Capacity (tons)	0.76	0.76	0.76	0.75	0.75
Total Capacity (tons)	2.30	2.40	2.42	2.44	2.49
Percent no filter Sensible Capacity	100.00%	106.35%	108.05%	109.73%	112.73%
Percent no filter Latent Capacity	100.00%	99.77%	99.32%	98.87%	98.64%
Percent no filter Total Capacity	100.00%	104.18%	105.17%	106.14%	108.07%

## REFERENCES

- Alnor Instruments. Retrieved from <http://www.alnor-usa.com>
- ANSI/ASHRAE (2007). ANSI/ASHRAE Standard 52.2. Method of testing general ventilation air-cleaning devices for removal efficiency by particle size. Atlanta, USA: American Society of Heating, Refrigerating and Air-Conditioning Engineers.
- ASHRAE. 2005. Chapter 35, “Duct Design.” *2004 ASHRAE Handbook—HVAC Systems and Equipment*. Atlanta: American Society of Heating, Refrigerating and Air-Conditioning Engineers, Inc.
- Atlanta Regional Commission (unknown). *Appendix: Housing*. Retrieved October 17, 2013 from <http://www.atlantaregional.com/land-use/housing>.
- Beaton, L. (personal communication, October 18, 2013).
- Brandemuehl MJ, Gabel S, Andersen I (1993). *A Toolkit for Secondary HVAC System Energy Calculation*. Atlanta, USA: American Society of Heating, Refrigerating and Air-Conditioning Engineers.
- Carrier Corporation. 1994. *Charging procedures for residential condensing units*. 020-122. Syracuse, NY. Carrier Corporation.
- Chimack, M., and D. Sellers. 2000. Using extended surface air filters in heating ventilation and air conditioning systems: Reducing utility and maintenance costs while benefiting the environment. In the *Proceedings of the 2000 ACEEE Summer Study on Energy Efficiency in Buildings* 3:77–88.
- Downey, T., and J. Proctor. 2002. What can 13,000 air conditioners tell us? In the *Proceedings of the 2002 ACEEE Summer Study on Energy Efficiency in Buildings* 1:53–67.
- Earnest, G.S., Chen, D., and Pui, David. Y. H. *An experimental study of filter loading with liquid aerosols (EPHB 218-05r)*. To be published in American Industrial Hygiene Association Journal.
- Fisk, W., D. Faulkner, J. Palonen, and O. Seppanen. 2002. Performance and costs of particle air filtration technologies. *Indoor Air* 12(4):223–34.

- International Code Council, *International Residential Code for One- and Two-Family Dwellings* (ICC, 2012).
- Murray, Matt, Fitzpatrick, Shawn. *Residential HVAC Electronically Commutated Motor Retrofit Report*. Advanced Energy, February 3<sup>rd</sup>, 2012.
- Nassif, Nabil. *The impact of air filter pressure drop on the performance of typical air-conditioning systems*. Building Simulation, Vol. 5, No. 4. (1 December 2012), pp. 345-350.
- Palani, M., D. O’Neal, and J. Haberl. 1992. The effect of reduced evaporator air flow on the performance of a residential central air conditioner. In the Proceedings of the 1992 Symposium on Building Systems in Hot-Humid Climates, pp. 20–26.
- Parker, D., J. Sherwin, R. Raustad, and D. Shirey III. 1997. Impact of Evaporator Coil Airflow in Residential Air-Conditioning Systems. *ASHRAE Transactions* 103(2):395-405.
- Proctor, J. 2012. *Residential AC Filters*. ASHRAE Journal.
- Rodriguez, A., D. O’Neal, M. Davis, and S. Kondepudi. 1996. *Effect of reduced evaporator airflow on the high temperature performance of air conditioners*. Energy and Buildings 24:195–201.
- Sachs, H., T. Kubo, S. Smith, and K. Scott. 2002. Residential HVAC fans and motors are bigger than refrigerators. In the *Proceedings of the 2002 ACEEE Summer Study on Energy Efficiency in Buildings* 1:261–72.
- Siegel, J., Walker, I., and Sherman, M., 2002. “Dirty Air Conditioners: Energy Implications of Coil Fouling.” *Proceedings of the 2002 ACEEE Summer Study on Energy Efficiency in Buildings*, 1 (2002), 287-300.
- Stephens, B., Novoselac, A., and Siegel, J.A. 2010. The effects of filtration on pressure drop and energy consumption in residential HVAC systems (RP-1299). *HVAC&R Research* 16(3), 273-294
- The Energy Conservatory. 2006. *TrueFlow® Air Handler Flow Meter Operation Manual*. Minneapolis, MN: The Energy Conservatory.

U.S. Census Bureau, Current Housing Reports, Series H150/09, *American Housing Survey for the United States: 2009*, U.S. Government Printing Office, Washington, DC, 20401.

Printed in 2011.

U.S. Energy Information Administration, Annual Energy Review 2011, DOE/EIA-0384 (2011), September 2012.

Yang, Li; Braun, James E.; and Groll, Eckhard A., "The Impact of Evaporator Fouling on the Performance of Packaged Air Conditioners" (2004). International Refrigeration and Air Conditioning Conference. Paper 687.